

***Electronic Supplementary Information (ESI)***

**Coordination disk-type nano-Saturn complexes**

Shun-Ze Zhan,<sup>\*ac</sup> Jing-Hong Li,<sup>a</sup> Guo-Hui Zhang,<sup>a</sup> Ming-De Li,<sup>a</sup> Shanshan Sun,<sup>a</sup> Ji Zheng,<sup>b</sup> Guo-Hong Ning,<sup>b</sup> Mian Li,<sup>a</sup> Dai-Bin Kuang,<sup>d</sup> Xu-Dong Wang,<sup>d</sup> and Dan Li<sup>\*b</sup>

<sup>a</sup> Department of Chemistry and Key Laboratory for Preparation and Application of Ordered Structural Materials of Guangdong Province, Shantou University, Shantou 515063, P. R. China

<sup>b</sup> College of Chemistry and Materials Science, Jinan University, Guangzhou 510632, P. R. China

<sup>c</sup> Chemistry and Chemical Engineering Guangdong Laboratory, Shantou 515031, P. R. China

<sup>d</sup> MOE Key Laboratory of Bioinorganic and Synthetic Chemistry, Lehn Institute of Functional Materials, School of Chemistry, Sun Yat-Sen University, Guangzhou 510275, P. R. China

Corresponding authors:

\*Email: [szzhan@stu.edu.cn](mailto:szzhan@stu.edu.cn) (S.Z.Z.).

\*Email: [danli@jnu.edu.cn](mailto:danli@jnu.edu.cn) (D.L.).

## Table of Contents

<b>1 Experimental Section .....</b>	<b>S2</b>
1.1 Materials and Measurements.....	S2
1.2 Synthesis .....	S2
1.3 Crystal Structure Determination.....	S2
<b>2 Results and Discussion.....</b>	<b>S3</b>
2.1 Summary of the related nano-Saturn structures.....	S3
2.2 Crystal Structures and Properties .....	S6
<b>3 Additional Theoretical Calculation Details.....</b>	<b>S17</b>
3.1 Density Functional Theory (DFT) calculation .....	S17
3.2 EDA calculation.....	S17
3.3 Calculated Results .....	S18
<b>4 Femtosecond Transient Absorption (fs-TA) .....</b>	<b>S27</b>
4.1 Reflectance Solid State UV-Vis-NIR Spectra.....	S27
4.2 Femtosecond Transient Absorption (fs-TA) Results .....	S28
<b>5 References.....</b>	<b>S29</b>

# 1 Experimental Section

## 1.1 Materials and Measurements

Commercially available chemicals were purchased and used without further purification. C<sub>60</sub> (99.5%) and C<sub>70</sub> (99.0%) were purchased from Xiamen Funano New Material Technology Company LTD. Infrared spectrum (IR) was obtained in KBr disk on a Nicolet Avatar 360 FTIR spectrometer in the range of 4000–400 cm<sup>-1</sup>; abbreviations used for the IR bands are: w = weak, m = medium, s = strong, vs = very strong. Elemental analysis (EA) of C, H, N was performed with an Elementar Vario EL III CHNS analyzer. Thermogravimetric analysis (TGA) was performed on a TA Instruments Q50 Thermogravimetric Analyzer under a nitrogen flow of 40 mL·min<sup>-1</sup> at a heating rate of 10 °C·min<sup>-1</sup>. Powder X-ray diffraction (PXRD) experiment was performed on a MiniFlex 600 X-ray diffractometer of Rigaku Corporation.

The diffuse reflectance solid-state UV-Vis spectra were recorded on a Lambda950 UV/Vis/NIR spectrophotometer of Perkin Elmer using pure powder sample on pure BaSO<sub>4</sub> background. In all cases, the crystalline sample was selected under a microscope with 40-time amplification. The phase purity of the samples is assured by elemental analysis and PXRD measurement.

The femtosecond transient absorption (fs-TA) spectroscopy was used to detect excited and transient states and its dynamics. The fs-TA spectra were recorded on a HELIOS Fire Transient absorption spectrometer (Ultrafast Systems) at the 1 kHz repetition rate and 100 fs time resolution, as described in literatures.<sup>[1]</sup> The sample was pumped by the visible light at 280 nm or 350 nm with the average power of 100 μW in order to possess enough energy to excite the C<sub>60</sub>-Saturn and C<sub>70</sub>-Saturn complexes, and the probe light was in the range of 800–1600 nm to cover the more absorbance of the sample.<sup>[1]</sup>

## 1.2 Synthesis

C<sub>60</sub>-Saturn ([Cu<sub>10</sub>(Mim)<sub>10</sub>] $\supset$ C<sub>60</sub>): A mixture of 2-Methylimidazole (8.2 mg, 0.1 mmol), C<sub>60</sub> (7.2 mg, 0.01 mmol), chlorobenzene (1.0 mL) and Copper trifluoroacetate hydrate (40 mg) in 0.2 mL 5% ammonia aqueous solution were sealed into a Pyrex tube. Then the tube was heated at 180 °C in a programmable oven for 72 h and cooled to room temperature at the rate of -5 °C/h. Black block crystals were obtained in 41.5% yield (based on C<sub>60</sub>). Anal. Calcd for C<sub>100</sub>H<sub>50</sub>Cu<sub>10</sub>N<sub>20</sub>: C, 55.42; H, 2.33; N, 12.93. Found: C, 55.31; H, 2.25; N, 12.79. IR data (KBr, cm<sup>-1</sup>): 3131 (w), 2906 (m), 1567 (s), 1463 (s), 1424 (s), 1367 (m), 1303 (s), 1184 (m), 1144 (s), 997 (m), 825 (w), 747 (s), 683 (m), 576 (w), 526 (m), 461 (w), 433 (w).

C<sub>70</sub>-Saturn ([Cu<sub>10</sub>(Mim)<sub>10</sub>] $\supset$ C<sub>70</sub>): A mixture of 2-Methylimidazole (8.2 mg, 0.1 mmol), C<sub>70</sub> (8.4 mg, 0.01 mmol), toluene (1.0 mL) and Copper trifluoroacetate hydrate (40 mg) in 0.2 mL 5% ammonia aqueous solution were sealed into a Pyrex tube. Then the tube was heated at 180 °C in a programmable oven for 72 h and cooled to room temperature at the rate of -5 °C/h. Black plate crystals were collected in about 10% yield. Anal. Calcd for C<sub>110</sub>H<sub>50</sub>Cu<sub>10</sub>N<sub>20</sub>: C, 57.77; H, 2.20; N, 12.25. Found: C, 57.69; H, 2.12; N, 12.06. IR data (KBr, cm<sup>-1</sup>): 3114 (w), 2906 (m), 1504 (w), 1463 (s), 1430 (s), 1367 (w), 1303 (m), 1186 (w), 1144 (s), 997 (w), 826 (w), 795 (w), 748 (s), 684 (w), 642(w), 577 (w), 536 (w), 457 (w).

## 1.3 Crystal Structure Determination

Single crystal X-ray data collection were performed on a Rigaku OD (Enhance Cu X-ray Source, K $\alpha$ ,  $\lambda$  = 1.54184 Å) with CCD Plate (XtaLAB Pro: Kappa single) at 300, 250, 200 and 100 K under cold dry N<sub>2</sub> atmosphere with a temperature controller. Data were processed with the CrysAlisPro 1.171.39.7e (Rigaku Oxford Diffraction, 2015). Structures were solved by direct methods (SHELXTL-97) and refined on F<sup>2</sup> using full-matrix last-squares (SHELXTL-97).<sup>[2]</sup> All non-hydrogen atoms were refined with anisotropic thermal parameters, and all hydrogen atoms were included in calculated positions and refined with isotropic thermal parameters riding on those of the parent atoms.

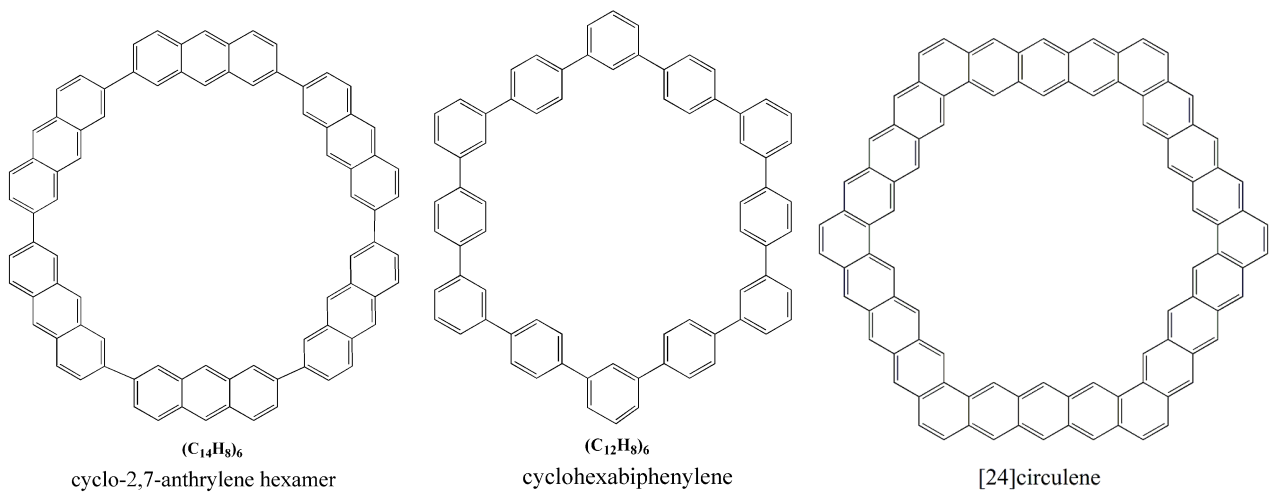
Crystal data and structure refinements were summarized in Table S2. Selected bond lengths and angles were given in Tables S3. CCDC 1943395-1943402 contain the supplementary crystallographic data for this paper.

## 2 Results and Discussion

### 2.1 Summary of the related nano-Saturn structures

**Table S1** Comparison of calculated interaction energy of various nano-Saturn systems based on different theoretical level.

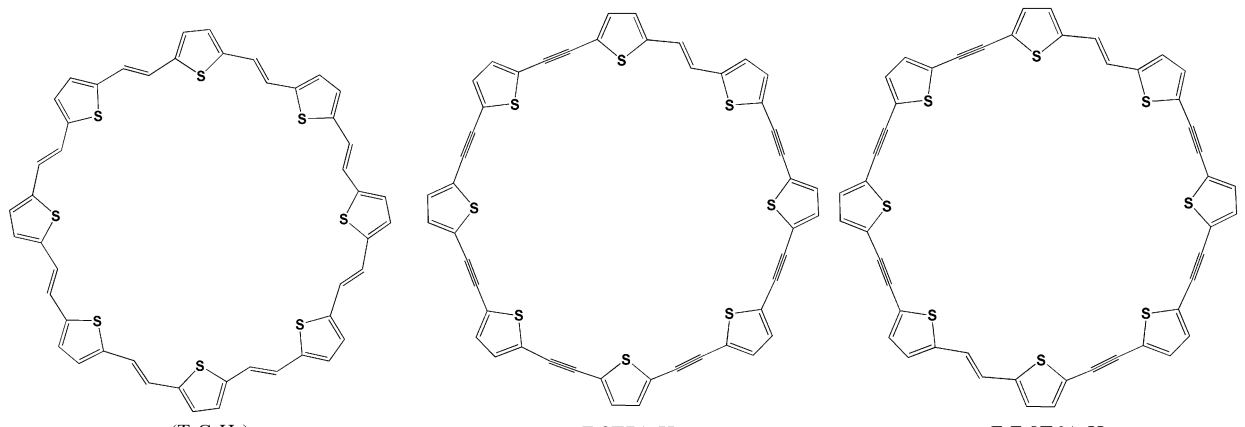
Nano-Saturn systems	$\Delta E(\text{kJ}\cdot\text{mol}^{-1})$	Theoretical level	References
<b>disk-type</b>			
[Cu <sub>10</sub> (Mim) <sub>10</sub> ] $\supset$ C <sub>60</sub>	-85.25	BLYP-D3(BJ)/TZP	This work
[Cu <sub>10</sub> (Mim) <sub>10</sub> ] $\supset$ C <sub>70</sub>	-116.07	BLYP-D3(BJ)/TZP	
(C <sub>14</sub> H <sub>8</sub> ) <sub>6</sub> $\supset$ C <sub>60</sub>	-56.7	M05-2X/6-31G(d) level	[3]
(C <sub>12</sub> H <sub>8</sub> ) <sub>6</sub> $\supset$ C <sub>60</sub> (staggered)	-58.83	vdW-DF2	[4]
[24]circulene $\supset$ C <sub>60</sub>	-51.11		[5]
(T-CC) <sub>8</sub> $\supset$ C <sub>60</sub>	-43.05	(M05-2X/6-311G(2d))	[6]
	-104.5	B3LYP-D3/6-311G(2d))	[6]
(T-C <sub>2</sub> H <sub>2</sub> ) <sub>8</sub> $\supset$ C <sub>60</sub>	-59.77	(M05-2X/6-311G(2d))	[6]
	-135.43	B3LYP-D3/6-311G(2d))	[6]
(T-CC) <sub>8</sub> $\supset$ C <sub>60</sub> 8T8A-H $\supset$ C <sub>60</sub>	-46.6	M06-2X/6-31G(d)	[7]
E,E-8T6A $\supset$ C <sub>60</sub>	-55.3		
E-8T7A $\supset$ C <sub>60</sub>	-51.6		
<b>belt-type</b>			
[12]CPP $\supset$ C <sub>60</sub> (staggered)	-61.72	vdW-DF2	[4]
[10]CPP $\supset$ C <sub>60</sub> (fivefold)	-132.51	(M05-2X/6-311G(2d))	[6]
	-248.71	B3LYP-D3/6-311G(2d))	
[10]CPP $\supset$ C <sub>60</sub> (sixfold)	-124.15	(M05-2X/6-311G(2d))	
	-240.77	B3LYP-D3/6-311G(2d))	
[12]CPP $\supset$ C <sub>60</sub>	-49.32	(M05-2X/6-311G(2d))	
	-127.49	B3LYP-D3/6-311G(2d))	
{[10]CPP $\supset$ Li@C <sub>60</sub> } <sup>+</sup> (fivefold)	-175.56	(M05-2X/6-311G(2d))	
	-282.57	B3LYP-D3/6-311G(2d))	
{[10]CPP $\supset$ Li@C <sub>60</sub> } <sup>+</sup> (sixfold)	-172.634	(M05-2X/6-311G(2d))	
	-280.06	B3LYP-D3/6-311G(2d))	
[10]CPP $\supset$ C <sub>60</sub>	-203.45	M062X/6-311G+(d,p)//M062X/6-31G(d)	[8]
[10]CPAq $\supset$ C <sub>60</sub>	-134.09 ~ -130.00	B97-D2/def2-TZVP level TURBOMOLE 6.3 program suite	[9]
[10]CPTcaq $\supset$ C <sub>60</sub>	-141.58 ~ -131.13		
[12]CPP $\supset$ C <sub>60</sub>	-131.46		
	-130.75		
[16]Cyclacene	-36.65	the STATE package	[10]
[17]Cyclacene	-128.27		
[18]Cyclacene	-109.94		
[19]Cyclacene	-64.61		
[20]Cyclacene	-35.68		



(a)

(b)

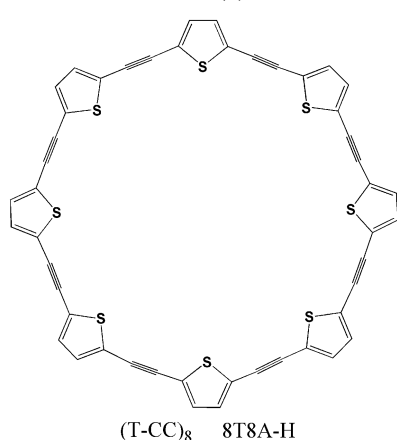
(c)



(d)

(e)

(f)



(g)

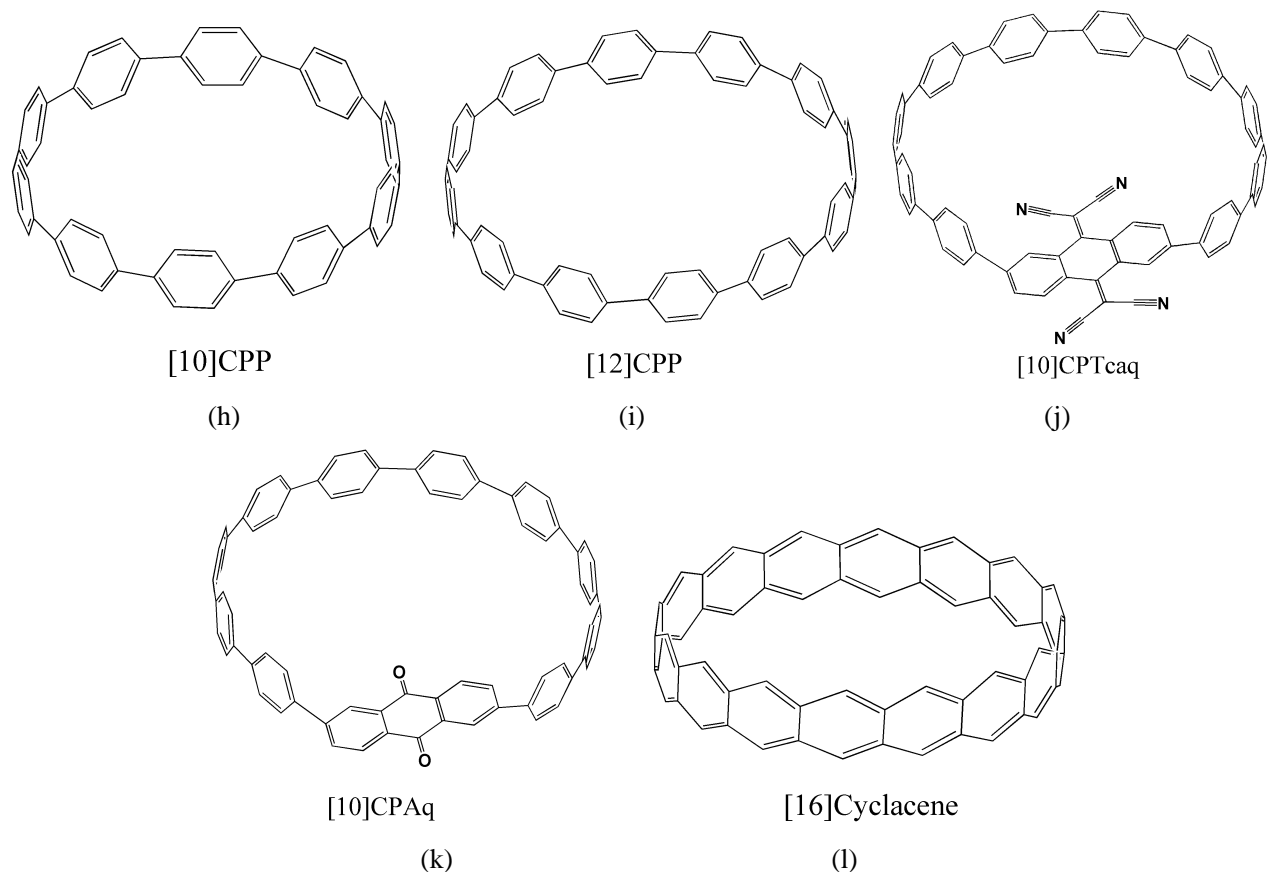


**Fig. S1** The well-reported organic macrocycles in the nano-Saturn system of Table S1. (a-g) disk-type macrocycles, (h-l) belt-type macrocycles.

## 2.2 Crystal Structures and Properties

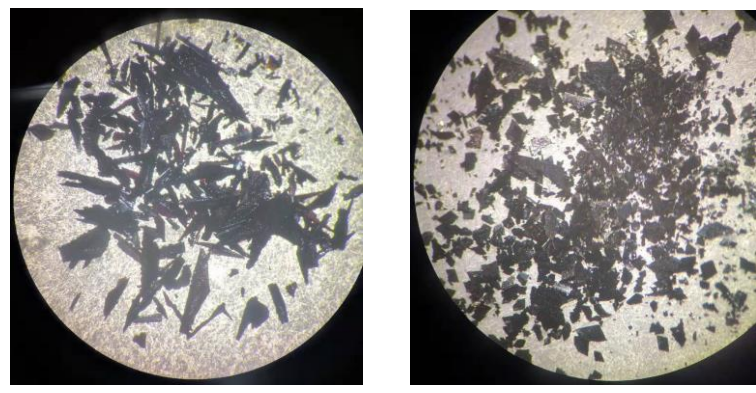
**Table S2** Crystal data and refinement parameters for the C<sub>60</sub>-Saturn and C<sub>70</sub>-Saturn.

Parameter	C <sub>60</sub> -Saturn				C <sub>70</sub> -Saturn			
Empirical formula	C <sub>100</sub> H <sub>50</sub> Cu <sub>10</sub> N <sub>20</sub>				C <sub>110</sub> H <sub>50</sub> Cu <sub>10</sub> N <sub>20</sub>			
Formula weight	2167.10				2287.10			
Temperature (K)	300	250	200	100	300	250	200	100
Crystal system	Monoclinic	Monoclinic	Triclinic	Triclinic	Triclinic	Triclinic	Triclinic	Triclinic
Space group	<i>C2/m</i>	<i>C2/m</i>	<i>P-I</i>	<i>P-I</i>	<i>P-I</i>	<i>P-I</i>	<i>P-I</i>	<i>P-I</i>
<i>a</i> (Å)	10.4531(2)	10.3986(3)	10.3877(2)	10.3306(4)	10.8776(2)	10.8822(2)	16.3006(3)	16.2846(2)
<i>b</i> (Å)	30.8052(6)	30.8174(8)	12.2263(3)	12.1908(6)	12.4524(1)	12.4297(2)	16.5127(3)	16.3744(1)
<i>c</i> (Å)	12.2818(2)	12.2534(3)	16.1951(4)	16.1323(6)	16.2822(2)	16.2388(3)	16.5388(2)	16.5641(1)
$\alpha$ (°)	90	90	90.741(2)	92.418(4)	95.700(1)	96.008(2)	98.050(1)	98.035(1)
$\beta$ (°)	91.966(2)	91.742(2)	107.985(2)	107.283(4)	108.748(1)	108.765(2)	98.473(1)	98.5660(1)
$\gamma$ (°)	90	90	91.592(2)	91.169(4)	91.392(1)	90.917(2)	108.223(2)	108.306(1)
<i>V</i> (Å <sup>3</sup> )	3952.53(13)	3924.88(18)	1955.07(8)	1937.06(15)	2074.41(5)	2065.44(7)	4099.39(13)	4063.82(7)
<i>Z</i>	2	2	1	1	1	1	2	2
<i>D</i> <sub>calcd</sub> (g/cm <sup>3</sup> )	1.821	1.834	1.841	1.858	1.831	1.839	1.853	1.869
$\mu$ (mm <sup>-1</sup> )	3.399	3.423	3.436	3.468	3.282	3.296	3.322	3.351
Reflections collected	16424	9946	18536	19096	40820	18849	67729	66609
Unique reflections	3379	3338	6524	7512	6968	6769	13809	13601
<i>R</i> <sub>int</sub>	0.0262	0.0270	0.0376	0.0376	0.0264	0.0173	0.0253	0.0265
GOOF on F <sup>2</sup>	1.088	1.084	1.051	1.089	1.046	1.094	1.045	1.093
<i>R</i> <sub>I</sub> [I ≥ 2σ(I)] <sup>[a]</sup>	0.0287	0.0447	0.0814	0.0756	0.0338	0.0316	0.0283	0.0284
<i>wR</i> <sub>2</sub> [I ≥ 2σ(I)] <sup>[b]</sup>	0.0842	0.1301	0.2228	0.2063	0.0940	0.0879	0.0804	0.0761
<i>R</i> <sub>1</sub> (all data) <sup>[a]</sup>	0.0308	0.0472	0.0892	0.0802	0.0341	0.0335	0.0300	0.0292
<i>wR</i> <sub>2</sub> (all data) <sup>[b]</sup>	0.0856	0.1323	0.2290	0.2085	0.0943	0.0894	0.0816	0.0767

<sup>[a]</sup> R<sub>1</sub> =  $\sum(|F_O| - |F_C|)/\sum|F_O|$ . <sup>[b]</sup> wR<sub>2</sub> =  $[\sum w(F_O^2 - F_C^2)^2 / \sum w(F_O^2)^2]^{1/2}$

**Table S3** Comparison of distances (Å) and angles (°) in the experimental (100 K) and optimized structures of the two nano-Sature complexes.

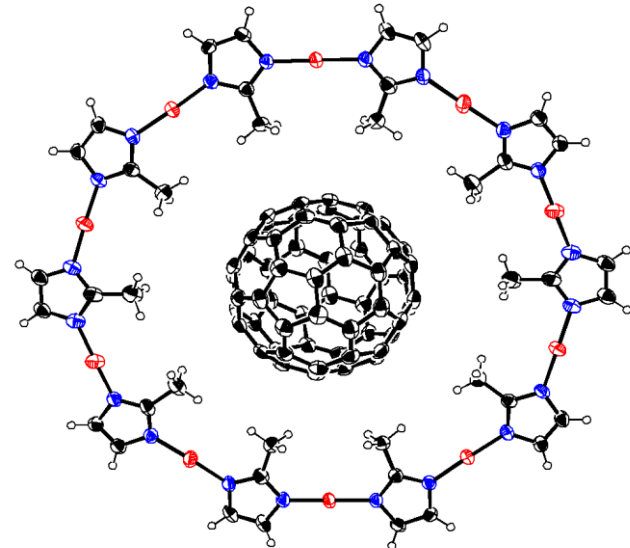
complexes	C <sub>60</sub> -Saturn		C <sub>70</sub> -Saturn		Cu <sub>10</sub> (Mim) <sub>10</sub>
	experimental	optimized	experimental	optimized	optimized
Cu-N	1.844(6) 1.848(6) 1.841(6) 1.841(6) 1.840(6) 1.847(6) 1.849(6) 1.846(6) 1.854(6) 1.856(6)	1.860~1.862	1.864(2) 1.863(2) 1.863(1) 1.861(2) 1.853(1) 1.858(2) 1.862(1) 1.865(1) 1.865(2) 1.863(1) 1.862(2) 1.861(2) 1.863(1) 1.857(1) 1.859(2) 1.855(1) 1.856(2) 1.858(2) 1.872(1) 1.871(2)	1.862~1.866	1.866
C(CH <sub>3</sub> )-fullerene	7.224(3) 7.095(2) 7.177(2) 7.077(2) 7.135(2)	7.160 7.165 7.188 7.262 7.188 7.159 7.211(7) 6.969(4) 7.167 7.187 7.262 7.186	7.502(6) 7.383(5) 7.121(8) 7.364(2) 7.353(1) 6.872 6.889 7.687 7.414 7.291(6) 7.502(1)	7.072 7.408 7.437 7.515 6.872 6.889 7.687 7.414 7.438 7.042	
opposite C(CH <sub>3</sub> )-C(CH <sub>3</sub> )	14.354(5) 14.190(5) 14.449(6) 14.270(5) 14.154(5)	14.375 14.331 14.319 14.374 14.524	14.835(1) 14.588(1) 14.090(1) 13.759(1) 14.648(1)	13.903 13.951 15.032 14.844 14.936	
center distances between the opposite Mim	19.385(8) 19.169(8) 19.637(8) 19.433(8) 19.592(8)	19.598 19.636 19.381 19.364 19.595	19.162(1) 18.961(1) 19.836(1) 19.787(1) 20.034(1)	19.698 19.096 18.421 19.040 20.096	21.347 19.259 16.943 18.283 20.853
dihedral angles between Mim and Cu plane	3.718(1) 5.454(2) 5.896(2) 10.530(4) 4.839(2) 3.718(1)	5.332 9.993 26.960 21.332 7.483 9.1622(8) 5.473 6.4337(5) 9.847 6.8739(6) 26.931 12.06(9) 21.449 6.84(9) 7.496 2.7247(2)	8.2169(7) 10.9272(9) 13.32(9) 8.30(9) 9.1622(8) 3.176 12.612 16.873 26.338 11.822 7.587	39.405 39.641 61.985 44.655 3.176 12.612 16.873 26.338 11.822 7.587	50.16 18.98 21.11 27.48 33.38
N-Cu-N	173.05(7) 175.31(7) 178.66(7) 178.10(7) 177.66(7)	178.56 177.29 178.78 178.48 178.13 178.52 177.30 178.73 178.55 178.11	177.05(8) 175.89(8) 172.25(8) 175.29(8) 178.97(8) 177.96(8) 175.75(8) 173.28(8) 175.57(8) 179.41(8)	179.53 177.24 178.43 175.19 175.74 178.06 175.17 176.80 178.74 176.89	177.05 177.24 174.36 176.51 179.03 177.05 177.24 174.36 176.51 179.03



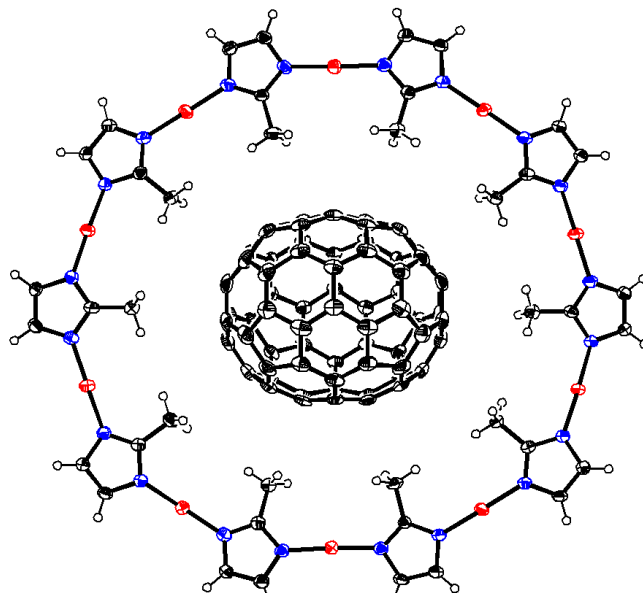
(a) C<sub>60</sub>-Saturn

(b) C<sub>70</sub>-Saturn

**Fig. S2** Crystal images of the two nano-Saturn complexes.

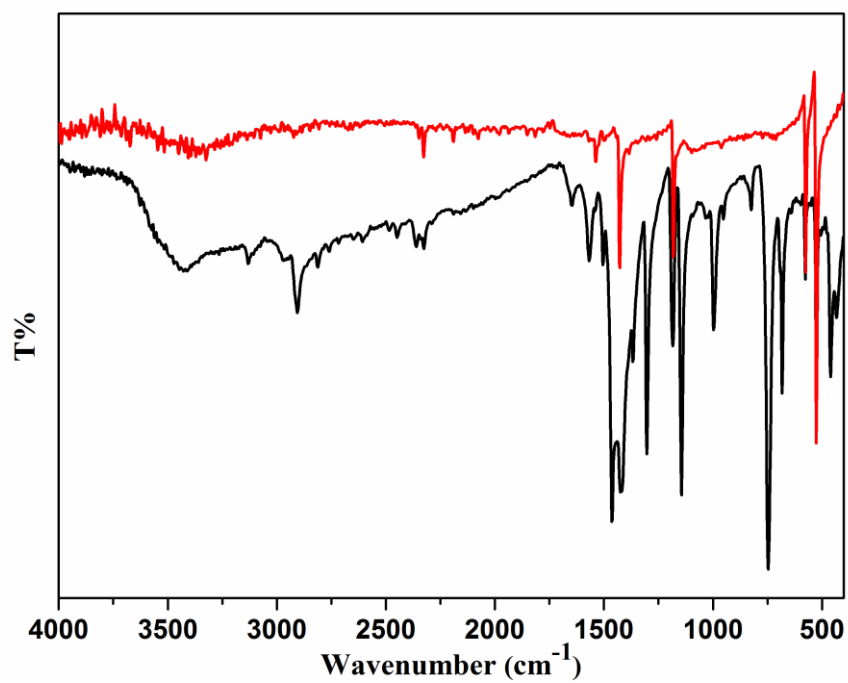


(a) C<sub>60</sub>-Saturn

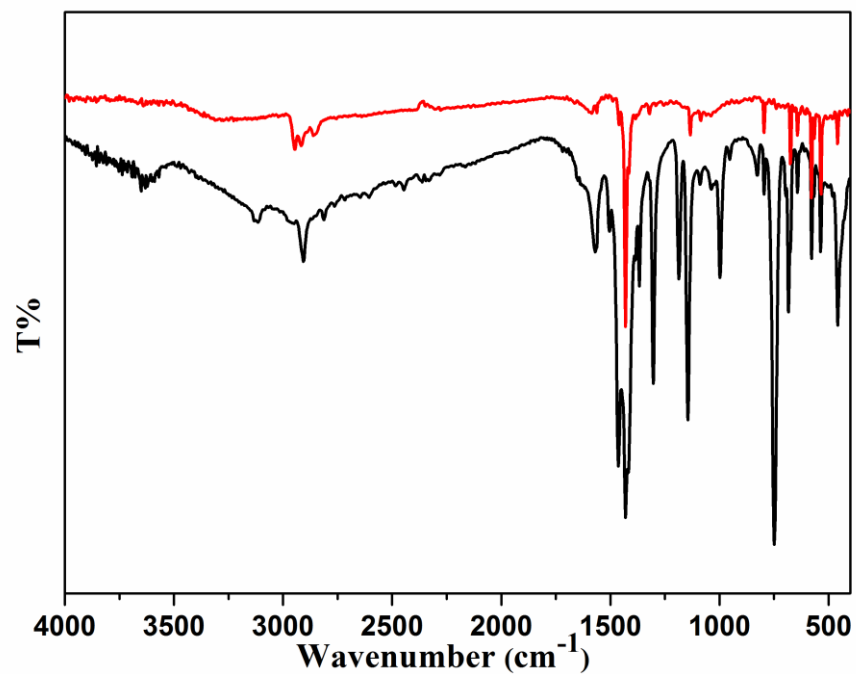


(b) C<sub>70</sub>-Saturn

**Fig. S3** Top view of the Saturn structures for the C<sub>60</sub>-Saturn (a) and C<sub>70</sub>-Saturn (b) with 50% thermal ellipsoid. Color codes: red, Cu; blue, N; black, C; white cycle, H.

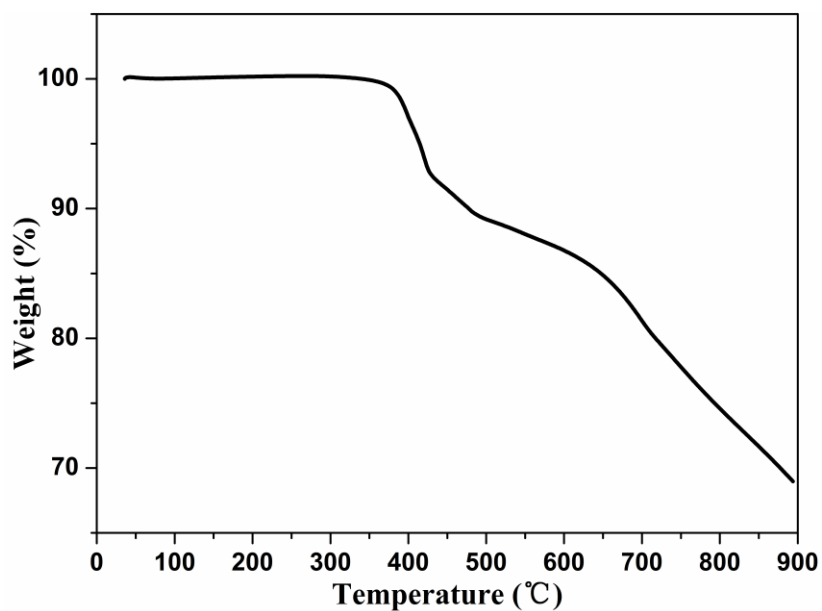


(a)  $\text{C}_{60}$  (red) and  $\text{C}_{60}$ -Saturn (black)

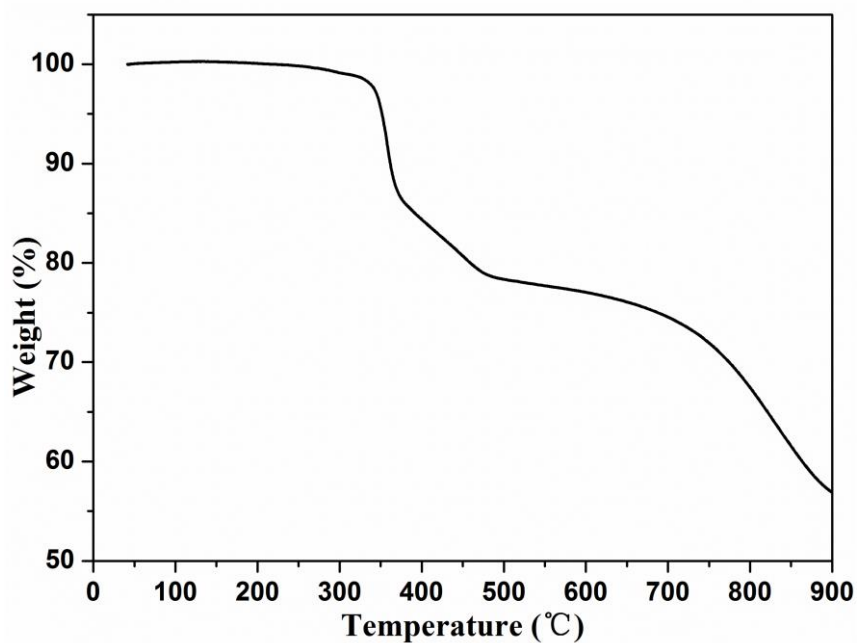


(b)  $\text{C}_{70}$  (red) and  $\text{C}_{70}$ -Saturn (black)

**Fig. S4** IR spectra of the fullerene ( $\text{C}_{60}$  and  $\text{C}_{70}$ , red) and nano-Saturn complexes (black).

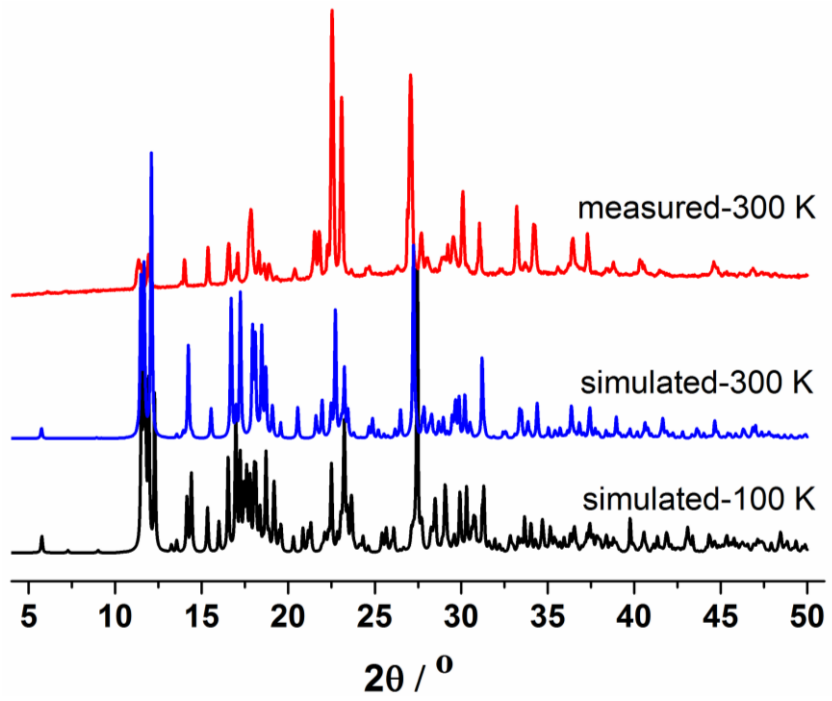


(a)  $\text{C}_{60}$ -Saturn

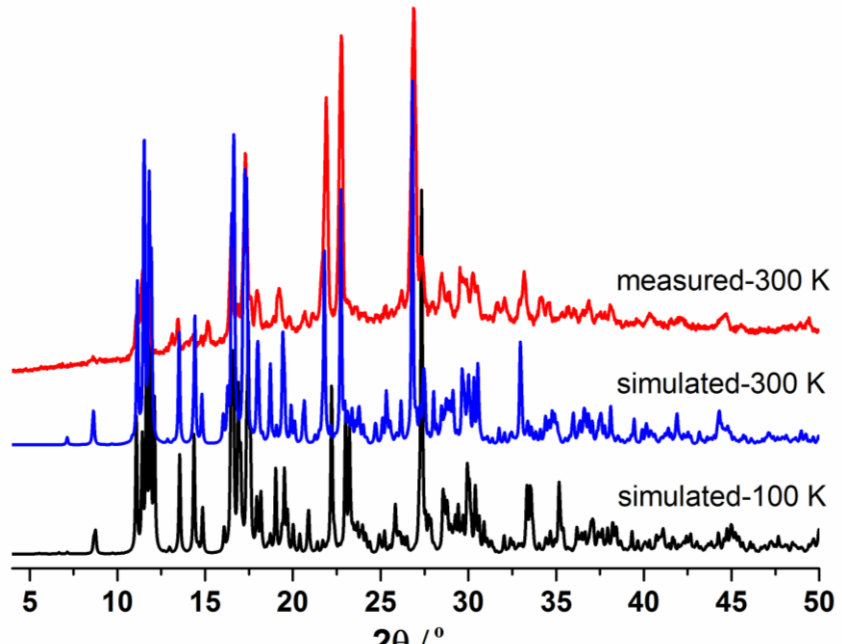


(b)  $\text{C}_{70}$ -Saturn

**Fig. S5** Thermogravimetric plots of the two nano-Saturn complexes.

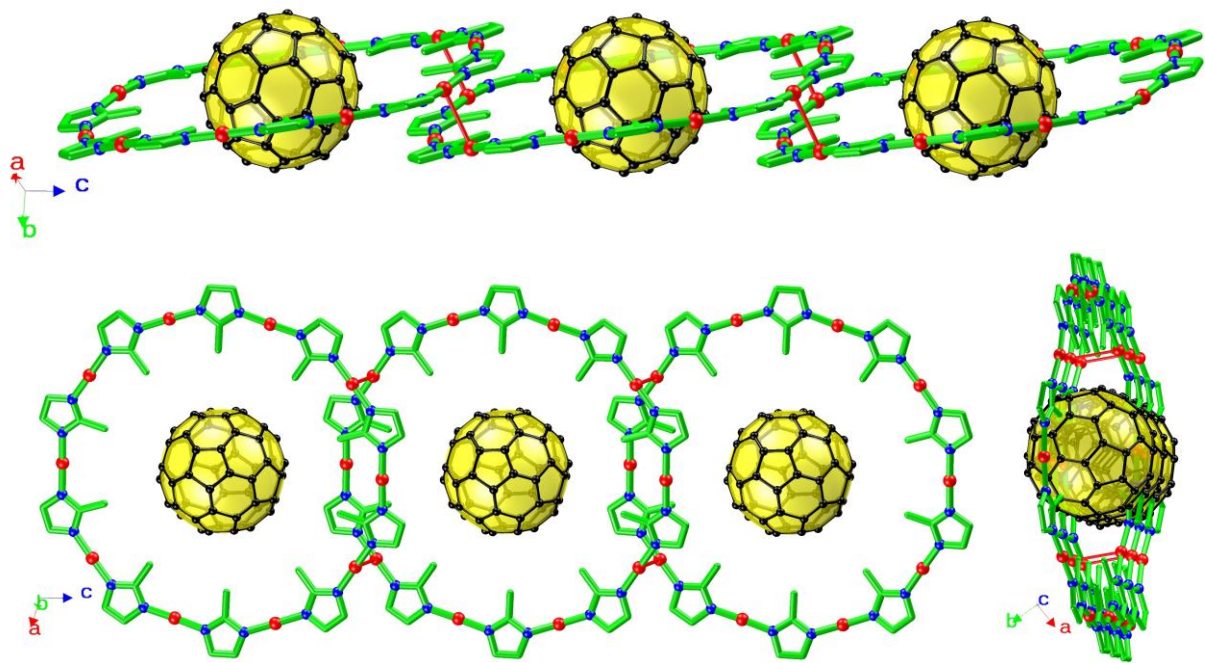


(a) C<sub>60</sub>-Saturn

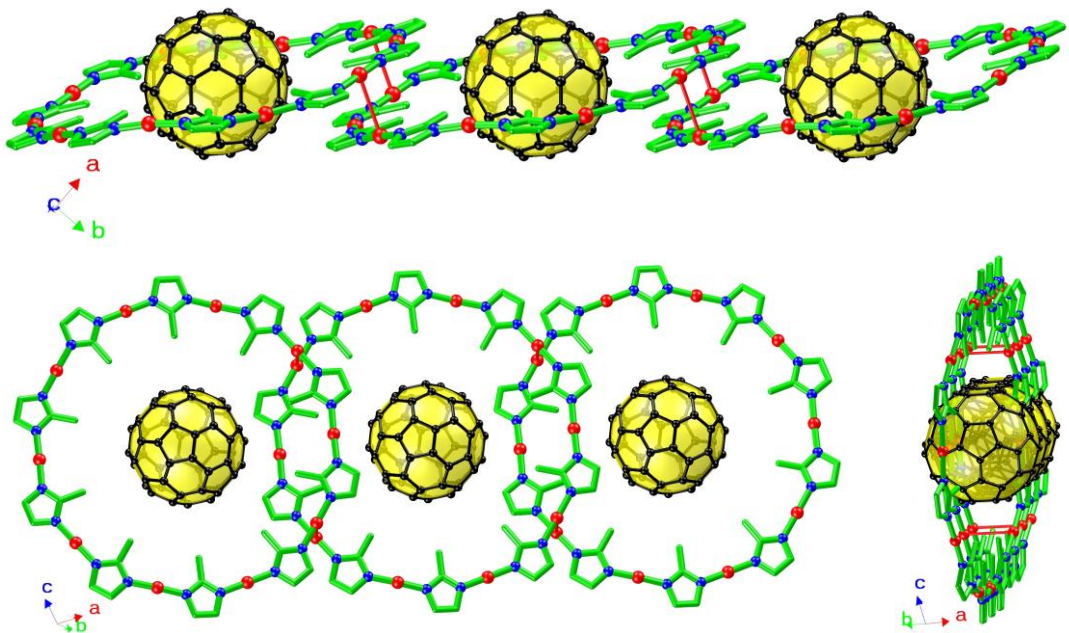


(b) C<sub>70</sub>-Saturn

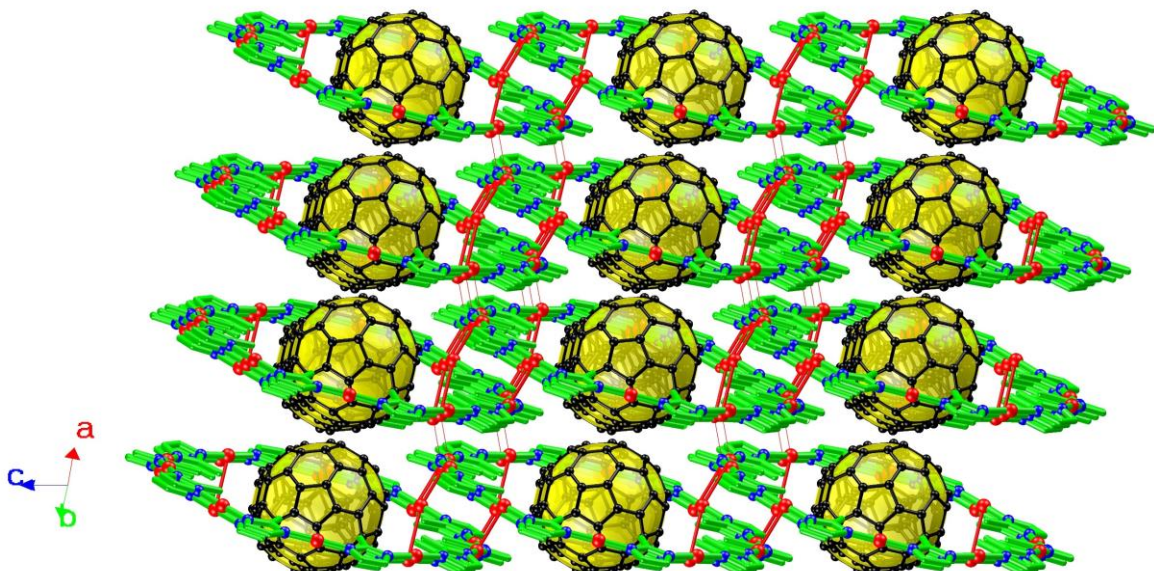
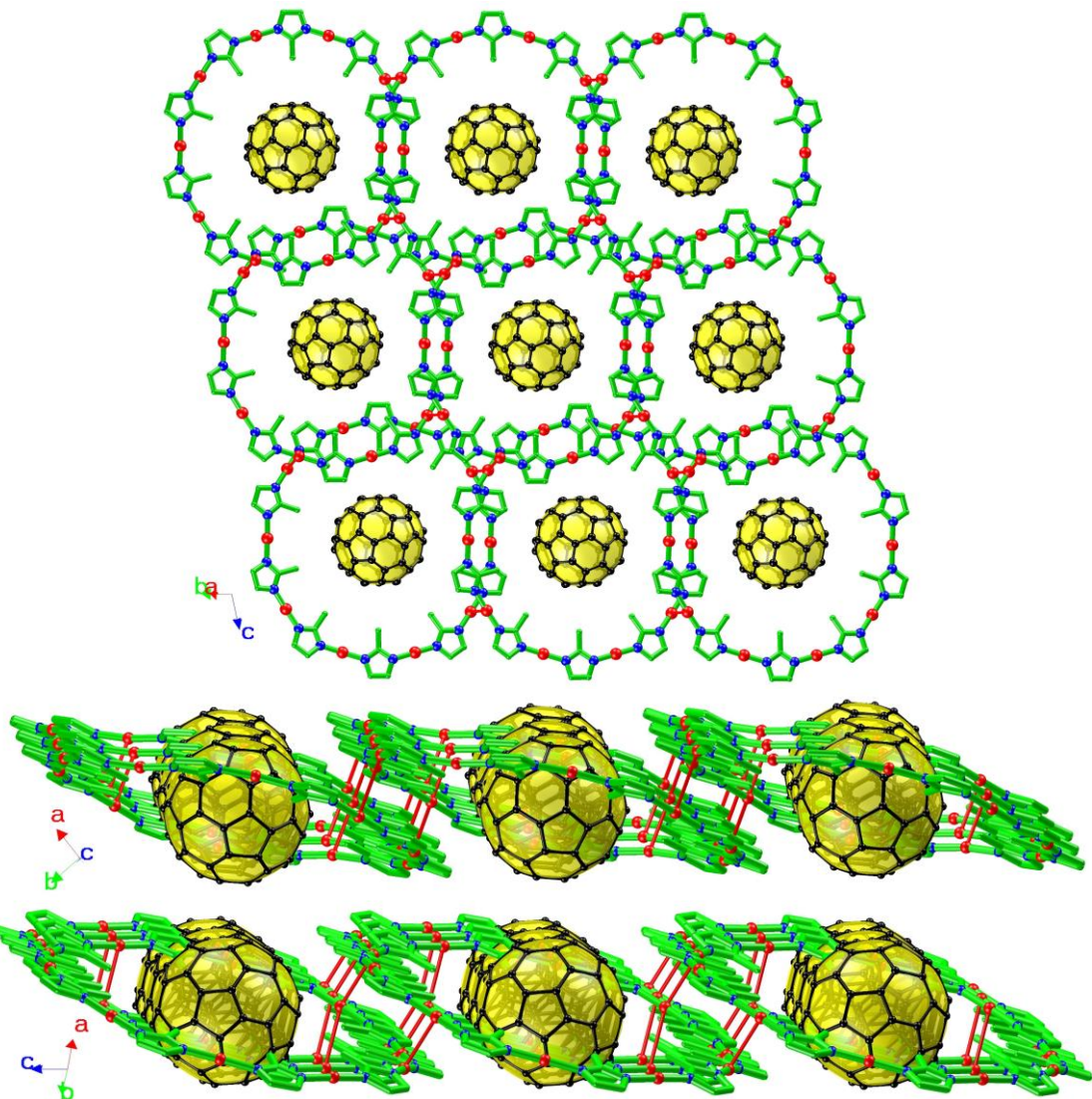
**Fig. S6** Comparison of the simulated and measured powder X-ray diffraction patterns of the nano-Saturn complexes. Note that: the measured PXRD pattern performed at 300 K (measured-300 K, red) is highly consistent with pattern of the simulated-300 K (blue), however, the simulated PXRD patterns with single crystal data at 300 K (simulated-300 K, blue) shows slight difference with that at 100 K (simulated-100 K, black) due to their different crystal system.

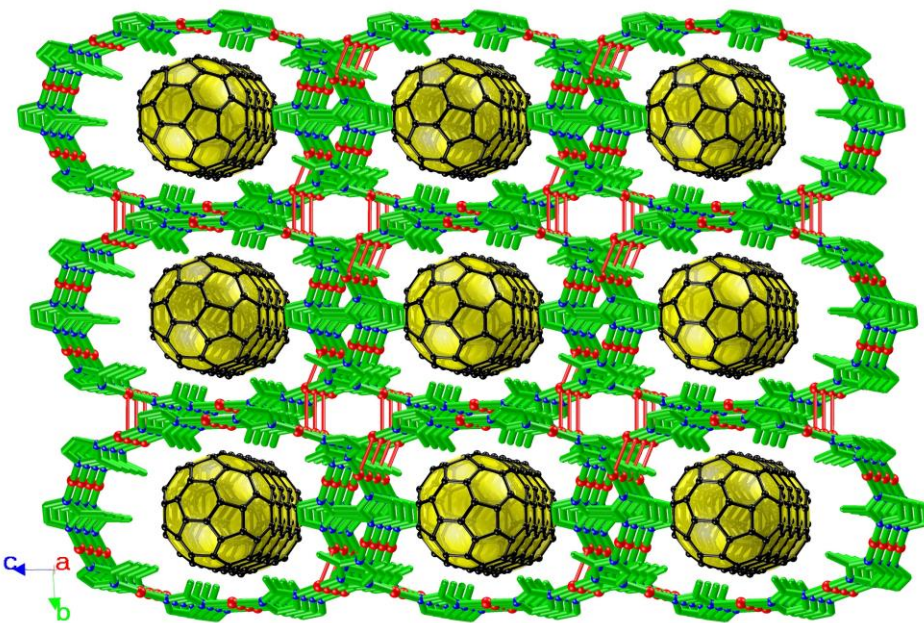


(a) 1-D chain along [001] direction (c axis) supported by a pair of Cu...Cu interactions (red bond,  $d_{\text{Cu...Cu}} = 3.021(1)$  Å) viewing from different orientations.



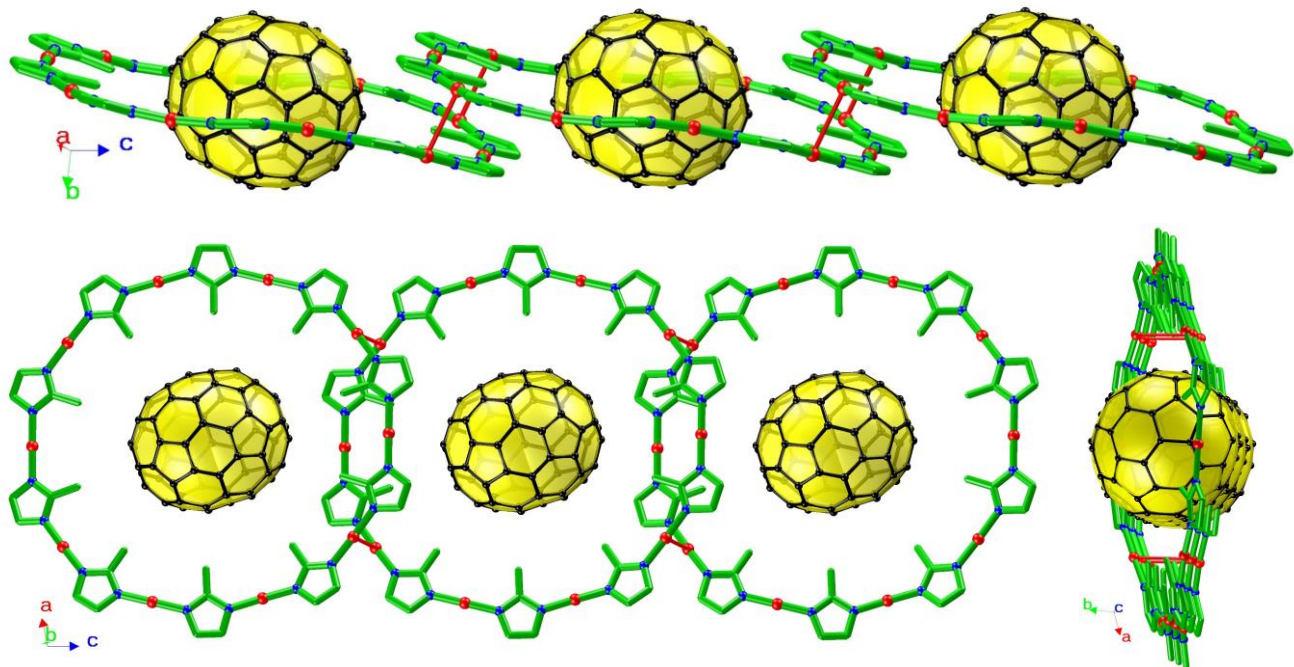
(b) 1-D chain along [110] direction supported by a pair of Cu...Cu interactions (red bond,  $d_{\text{Cu...Cu}} = 3.166(1)$  Å) viewing from different orientations.



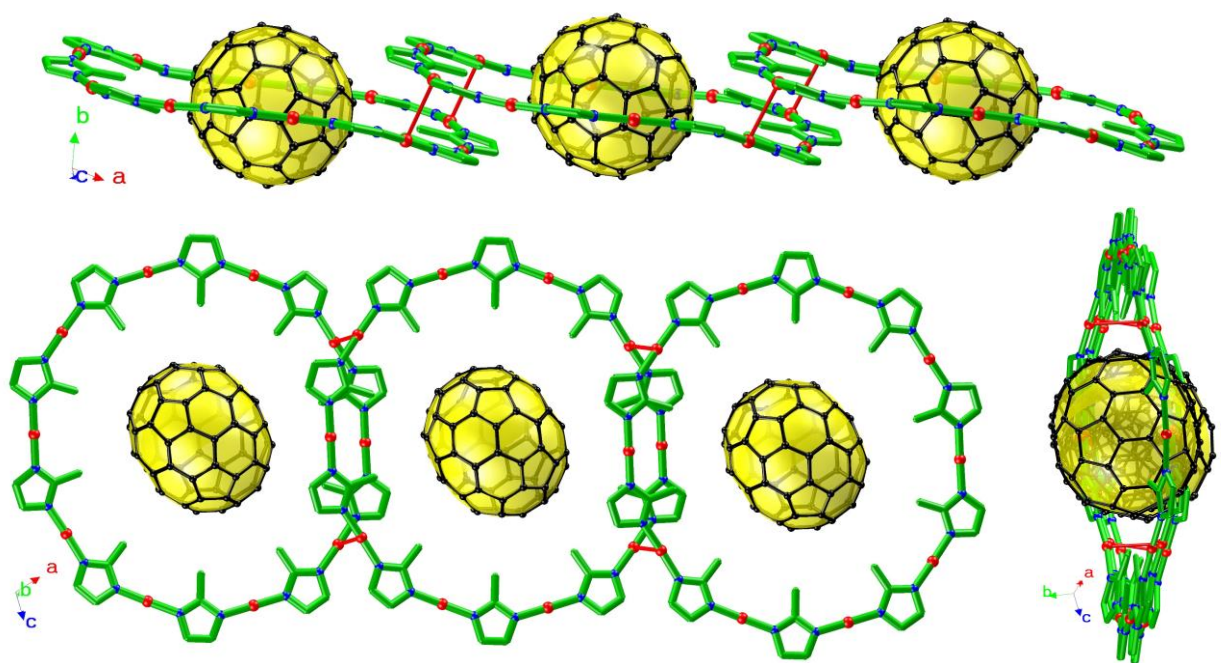


(e) 3-D stacking structure showing the 1-D channel along *a* axis.

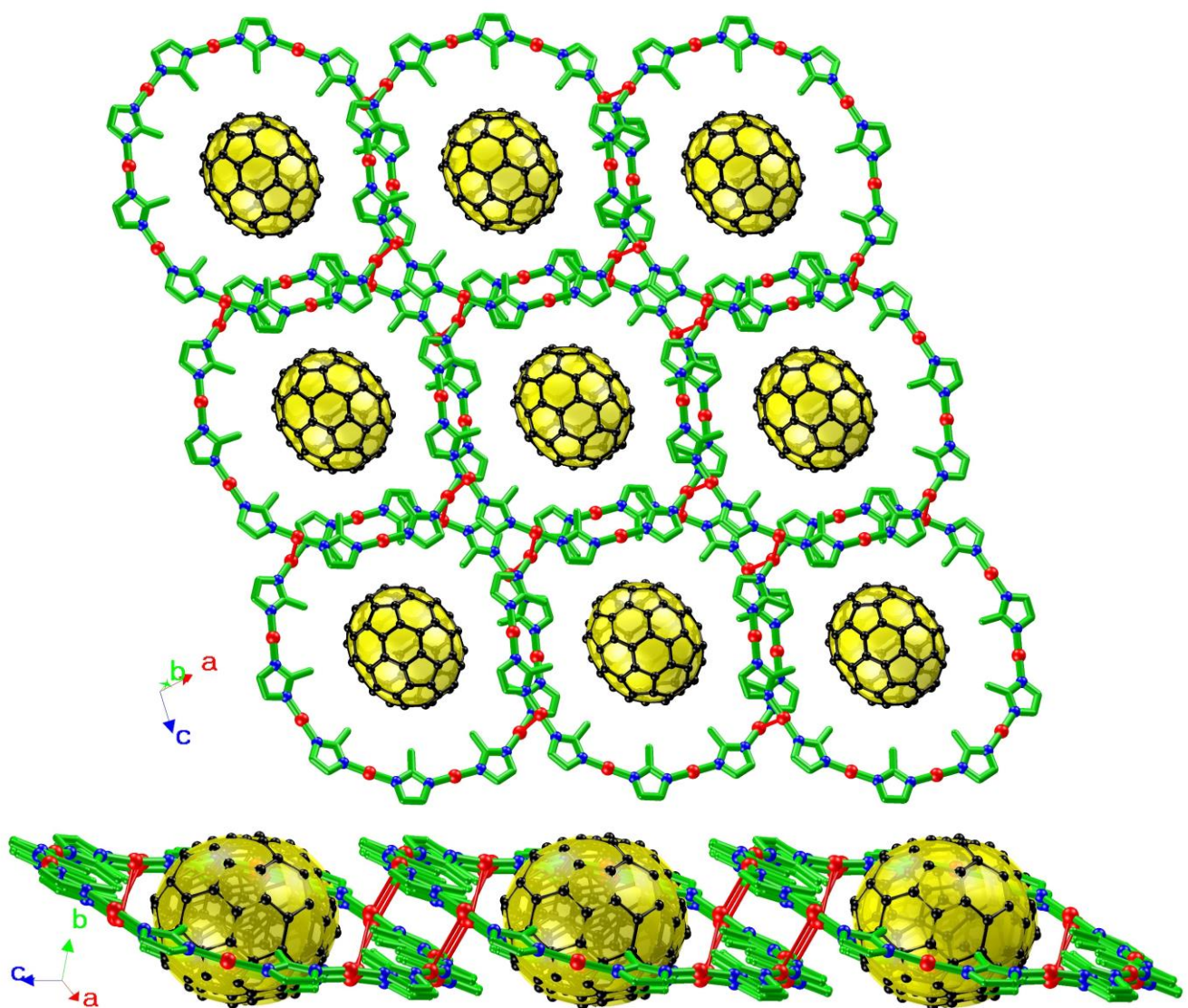
**Fig. S7** Stacking structure of the C<sub>60</sub>-Saturn complex.



(a) 1-D chain along [001] direction (*c* axis) supported by a pair of Cu···Cu interactions (red bond,  $d_{\text{Cu}\cdots\text{Cu}} = 3.129(4)$  and  $3.039(4)$  Å) viewing from different orientations.



(b) 1-D chain along [211] direction supported by a pair of Cu...Cu interactions (red bond,  $d_{(\text{Cu}\cdots\text{Cu})} = 3.037(1)$  and  $3.040(1)$  Å) viewing from different orientations.



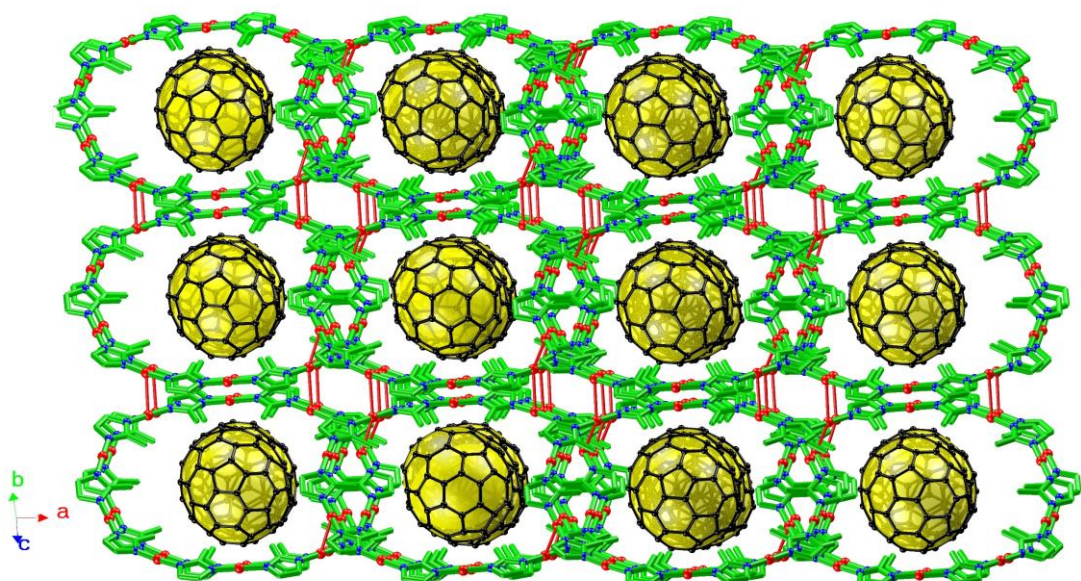
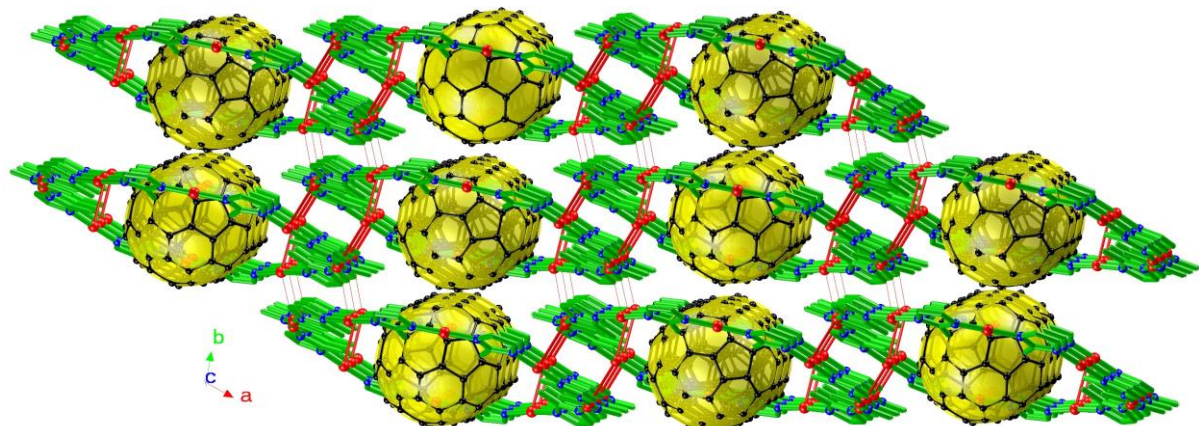
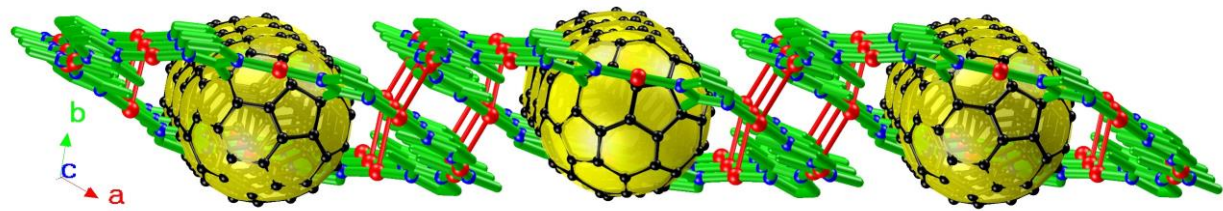


**Fig. S8** Stacking structure of the C<sub>70</sub>-Saturn complex.

### 3 Additional Theoretical Calculation Details

#### 3.1 Density Functional Theory (DFT) calculation

Quantum chemical calculations were carried out using Density Functional Theory (DFT) methods as implemented in the Amsterdam Density Functional (ADF 2016)<sup>[11-13]</sup> program package and Gaussian 09 software package.<sup>[14]</sup>

The geometrical structures of the two nano-Saturn complexes were optimized using ADF program package with auto symmetry constrains. The generalized gradient approximation (GGA) with the BLYP-D3(BJ) exchange-correlation functional<sup>[15]</sup> was employed, together with the TZP Slater basis sets for all the atoms.<sup>[16]</sup> Small frozen core approximations were applied to the inner shells for all atoms. The scalar relativistic (SR) effects were taken into account by the zero-order-regular approximation (ZORA).<sup>[17]</sup>

To analyse the molecular electrostatic potential (MEP) surface and molecular orbital (MO), the single point energy of the two nano-Saturn complexes were calculated by Gaussian 09 software package,<sup>[14]</sup> and some of the output files were used as input files of Multiwfn software packages<sup>[18]</sup> to perform wave function analysis. PBE0 functional<sup>[19-21]</sup> was used throughout, and LANL2DZ basis set<sup>[22]</sup> was used for Cu atoms while the 6-31G\*\* basis set<sup>[23]</sup> was employed for other atoms (C, N and H).

#### 3.2 EDA calculation

To make a further comprehend into host-guest interactions in the two nano-Saturns, we evaluated the energy of the interaction ( $\Delta E_{\text{int}}$ ) between the macrocycle and fullerene planet in terms of different chemically meaningful quantities within energy decomposition analysis (EDA) proposed by Ziegler and Rauk.<sup>[24-26]</sup>  $\Delta E_{\text{int}}$  can be decomposed into four quantities according to:

$$\Delta E_{\text{int}} = \Delta E_{\text{Pauli}} + \Delta E_{\text{elstat}} + \Delta E_{\text{orb}} + \Delta E_{\text{disp}}$$

where the  $\Delta E_{\text{Pauli}}$  part concerns the nature of destabilization owing to the four-electron/two-orbital repulsion between occupied orbitals from the different moieties. The  $\Delta E_{\text{elstat}}$  and  $\Delta E_{\text{orb}}$  interpret the favorable electrostatic and covalent character of the interaction. Furthermore, the dispersion interaction ( $\Delta E_{\text{disp}}$ ) was evaluated via the pairwise correction of Grimme<sup>[27]</sup> (DFT-D3), indicating a stabilizing character.

The EDA calculation was performed using the ADF2016 code.<sup>[11-13]</sup> Triple- $\xi$  and one polarization functions (STO-TZP) basis sets were employed within the generalized gradient approximation(GGA) of BLYP exchange–correlation functional. The pair-wise Grimme correction (D3)<sup>[28-30]</sup> and Becke–Johnson damping functions<sup>[31-32]</sup> were considered for the empirical dispersion correction to density functional theory (DFT-D). The geometry-optimized nano-Saturn structure were used for calculation.

### 3.3 Calculated Results

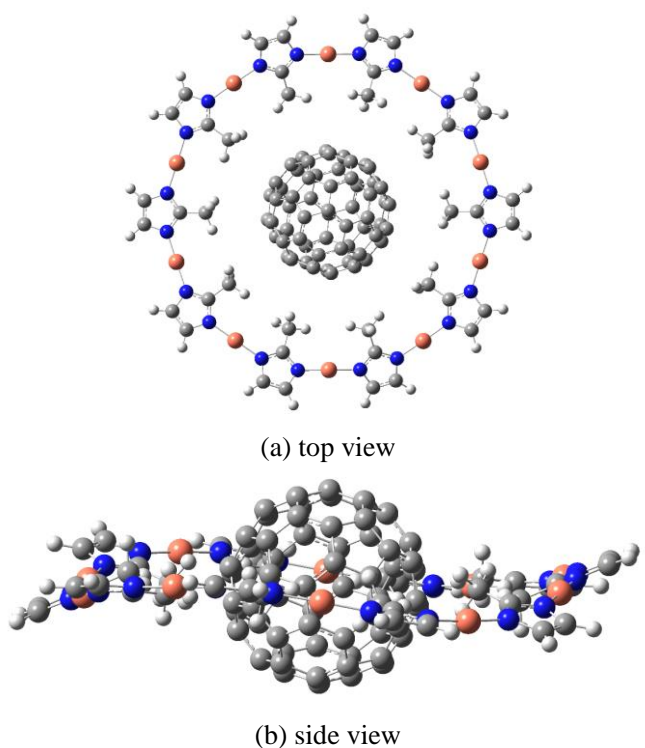


**Fig. S9** Optimized structure of the C<sub>60</sub>-Saturn.

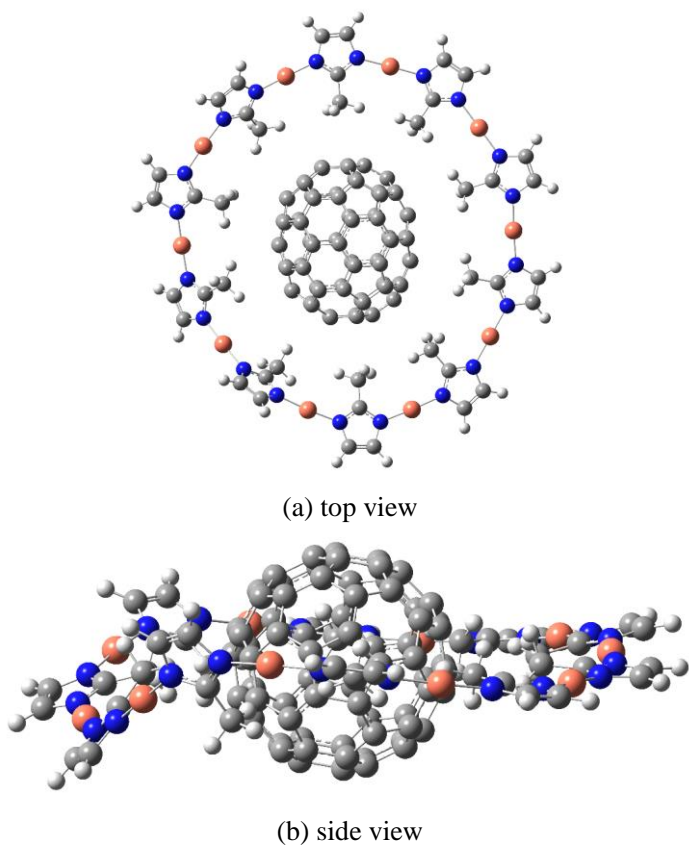
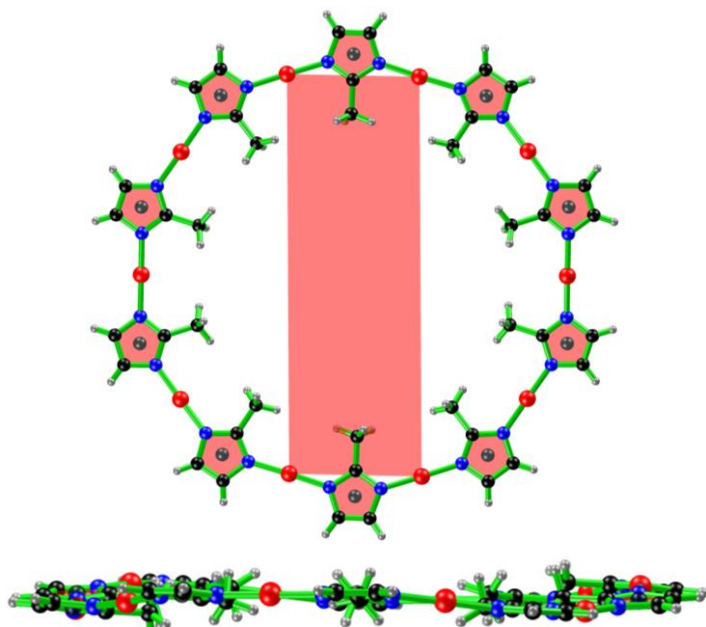
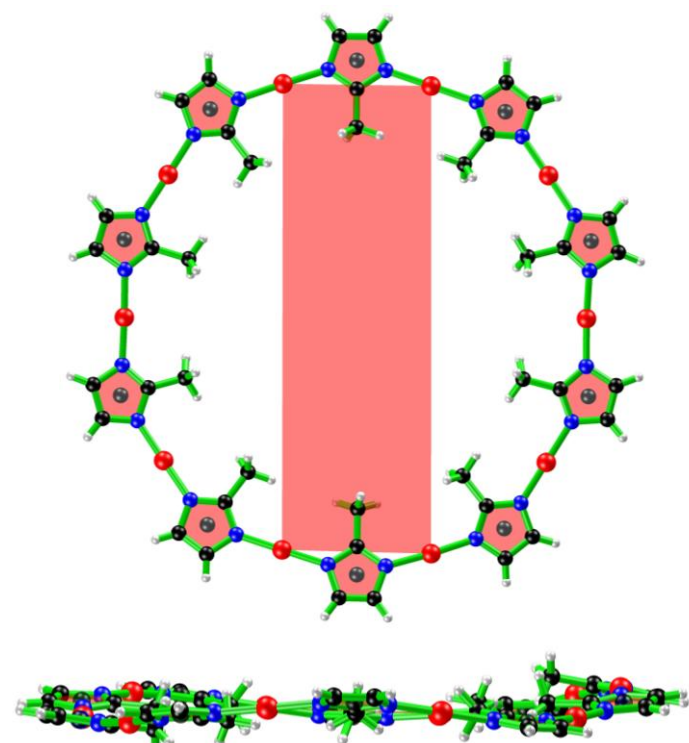


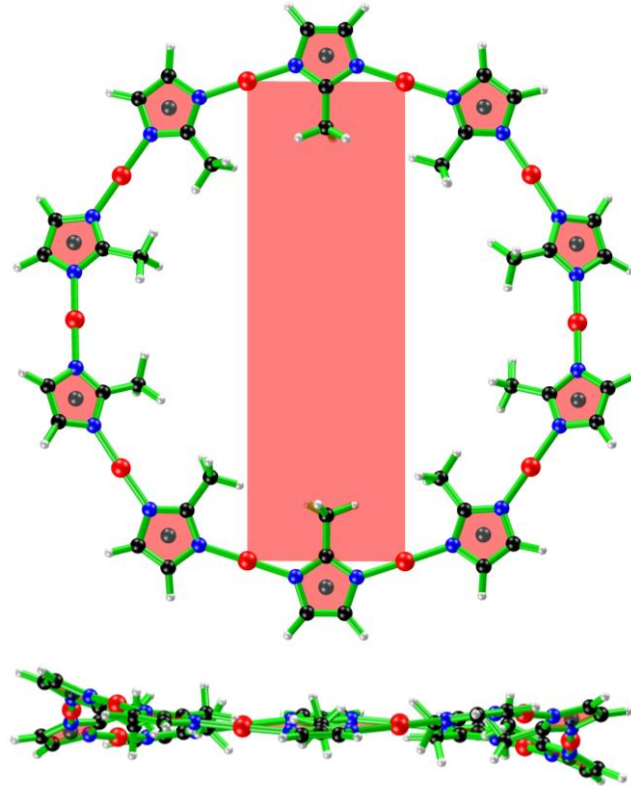
**Fig. S10** Optimized structure of the C<sub>70</sub>-Saturn.



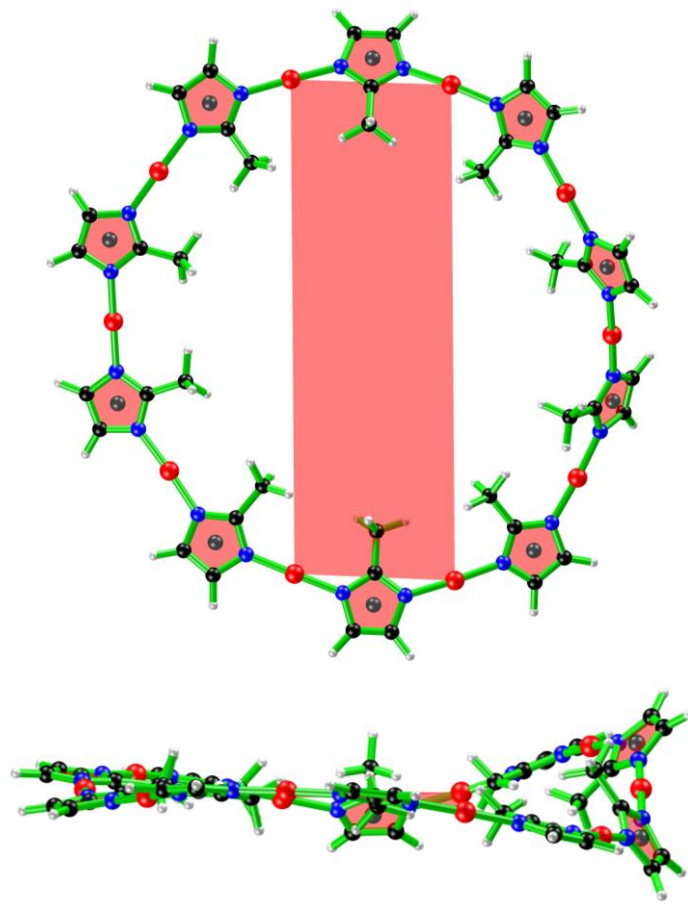
(a) [Cu<sub>10</sub>(Mim)<sub>10</sub>] in the C<sub>60</sub>-Saturn



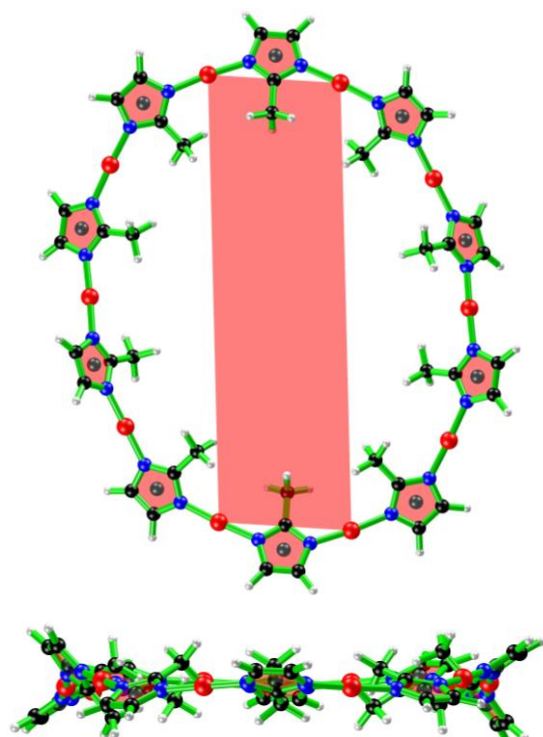
(b) [Cu<sub>10</sub>(Mim)<sub>10</sub>] in the C<sub>70</sub>-Saturn



(c)  $[\text{Cu}_{10}(\text{Mim})_{10}]$  in the optimized  $\text{C}_{60}$ -Saturn



(d)  $[\text{Cu}_{10}(\text{Mim})_{10}]$  in the optimized  $\text{C}_{70}$ -Saturn



(e) Optimized free  $[\text{Cu}_{10}(\text{Mim})_{10}]$

**Fig. S11** Comparison of the structures of the coordination macrocycles in (a) C<sub>60</sub>-Saturn, (b) C<sub>70</sub>-Saturn, (c) optimized C<sub>60</sub>-Saturn, (d) optimized C<sub>70</sub>-Saturn and (e) optimized free [Cu<sub>10</sub>(Mim)<sub>10</sub>] from top view (top) and side view (bottom). Note that the macrocycle plane is represented by the Cu<sub>4</sub> plane.

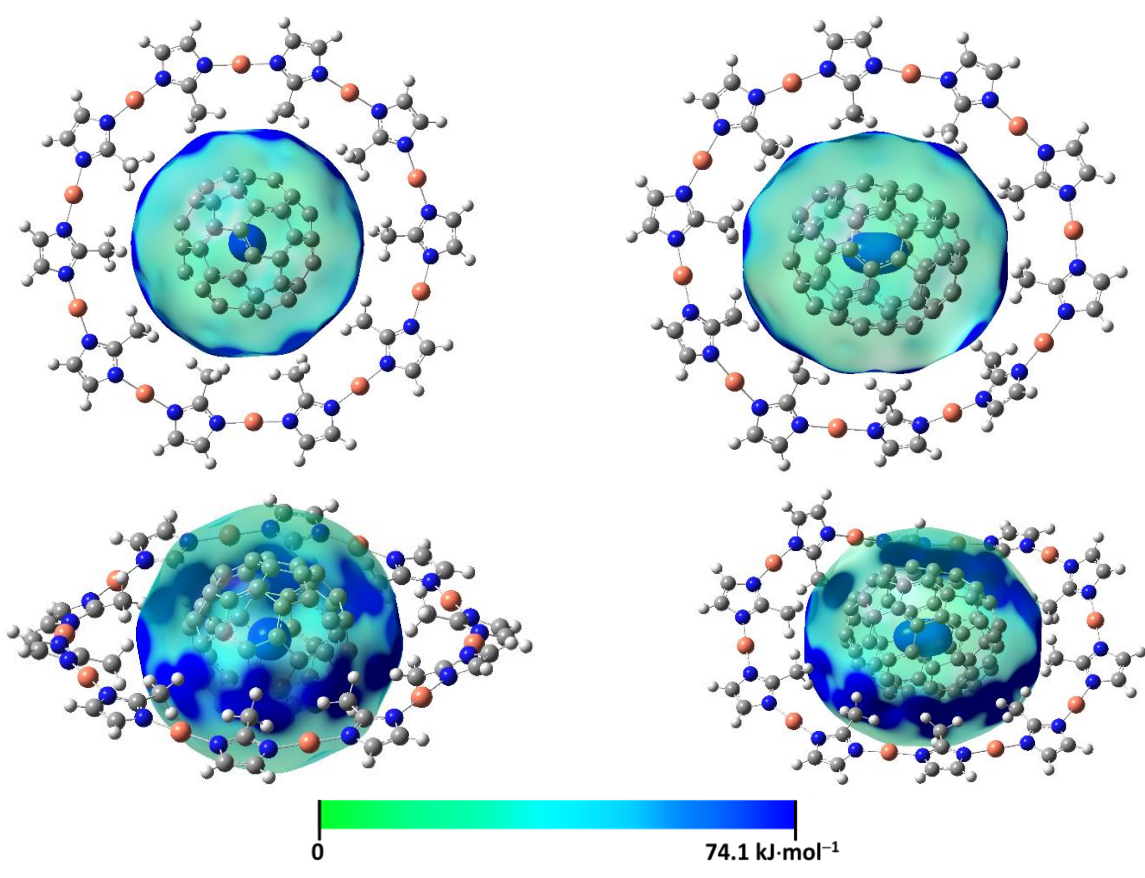
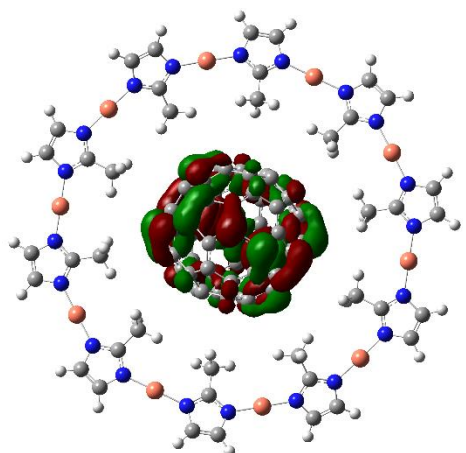
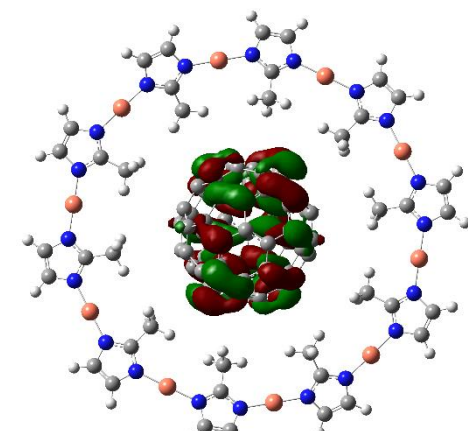


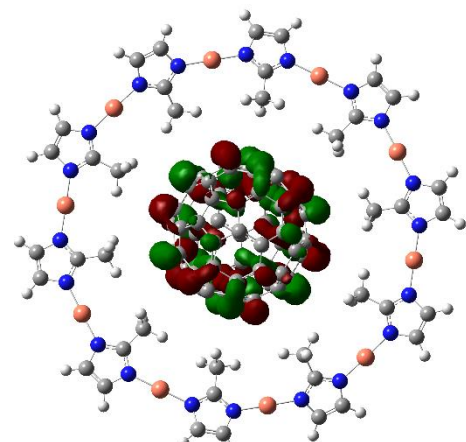
**Fig. S12** MEP surface at C<sub>60</sub> surface in the C<sub>60</sub>-Saturn (a) and C<sub>70</sub> surface in the C<sub>70</sub>-Saturn (b) from top view (top) and



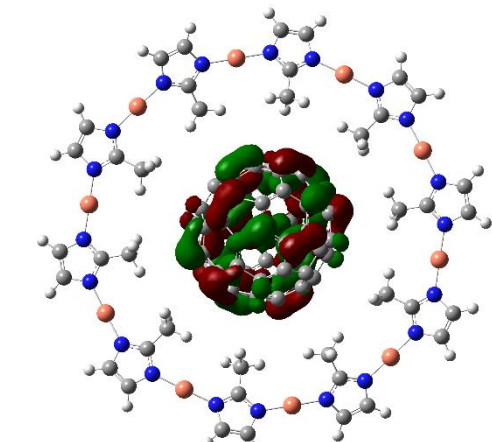
(a) LUMO+5



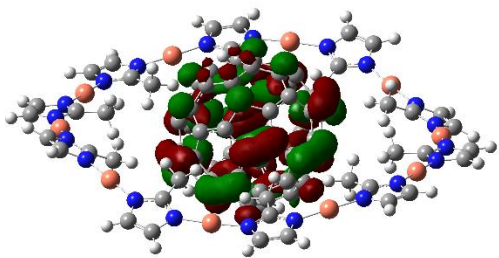
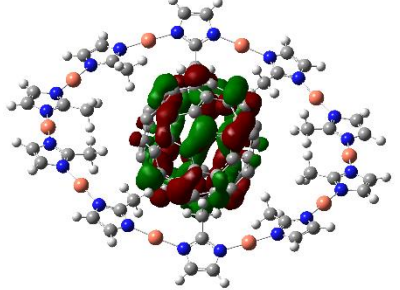
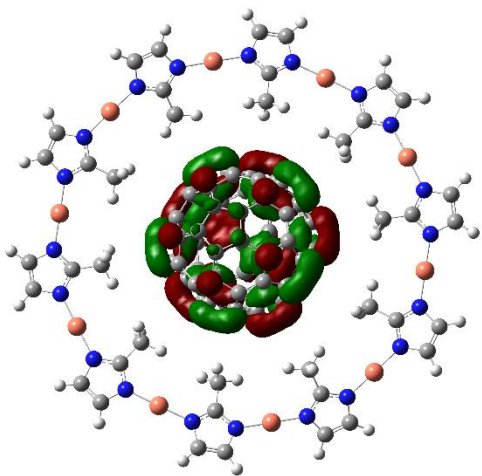
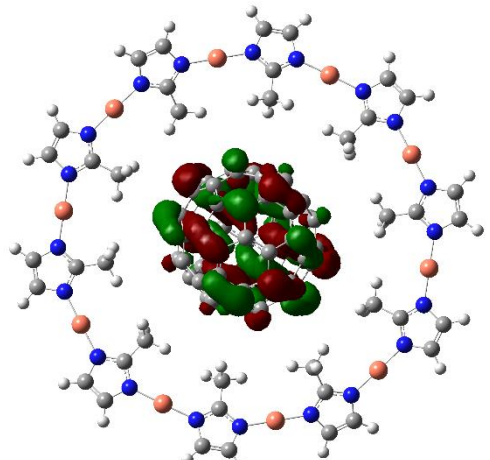
(b) LUMO+4



(c) LUMO+3

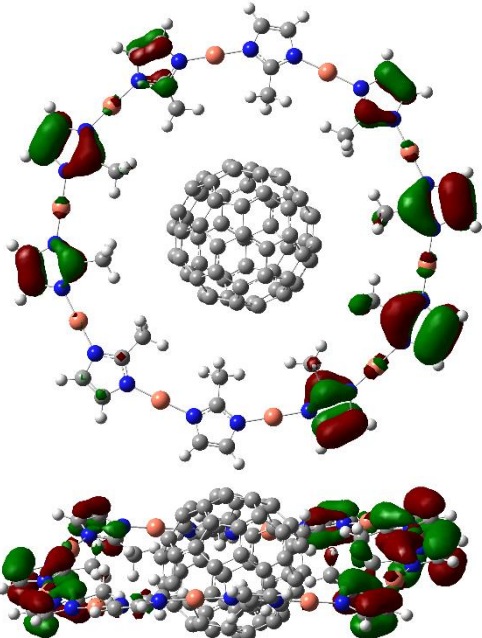
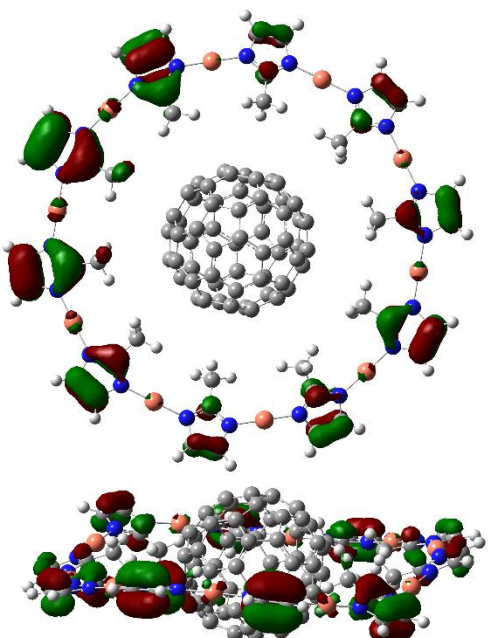


(d) LUMO+2



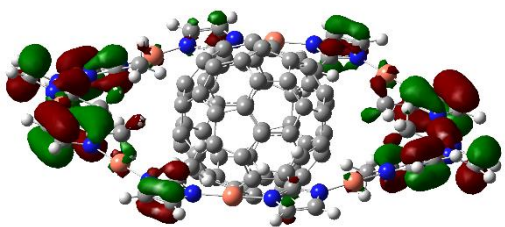
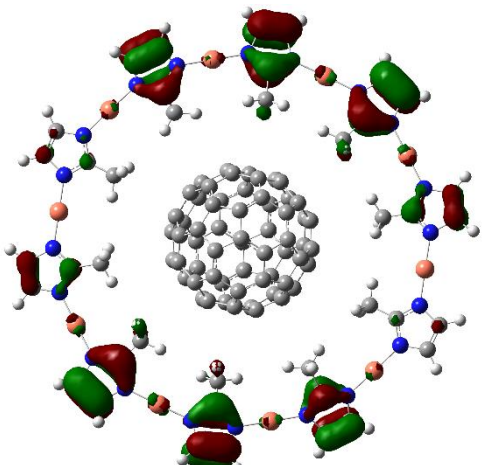
(e) LUMO+1

(f) LUMO

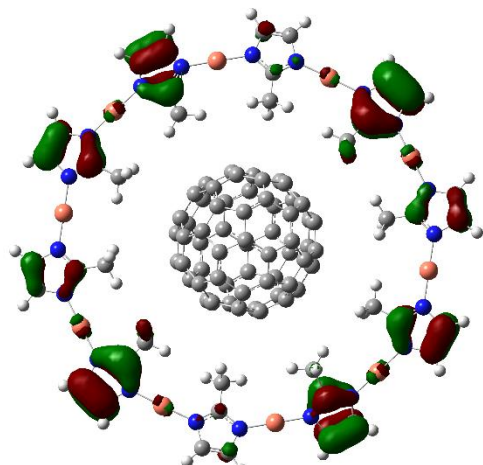


(g) HOMO

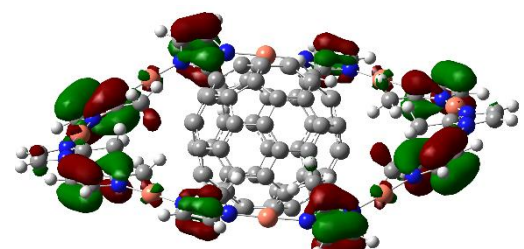
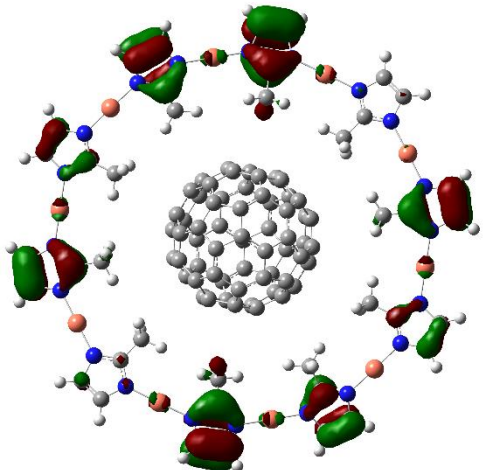
(h) HOMO-1



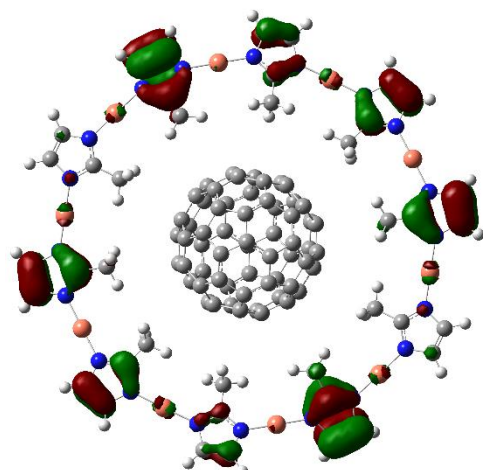
(i) HOMO-2



(j) HOMO-3

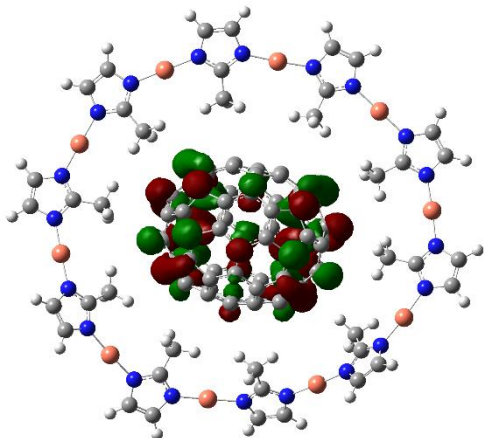


(k) HOMO-4

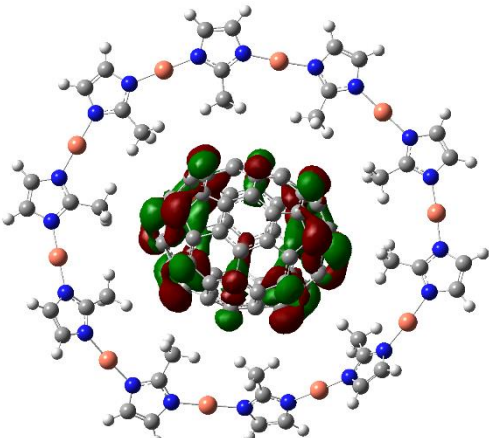


(l) HOMO-5

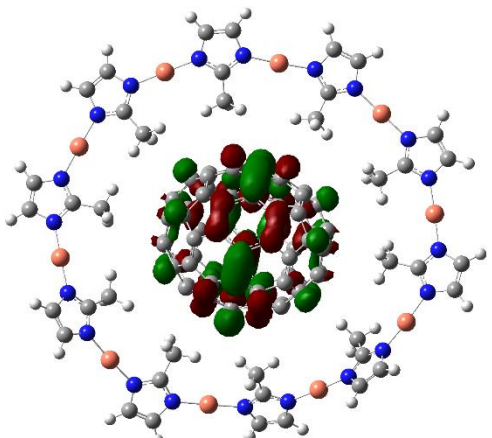
**Fig. S13** Selected molecular orbitals (MOs) at the PBE0 level of theory for the C<sub>60</sub>-Saturn (isovalue = 0.015).



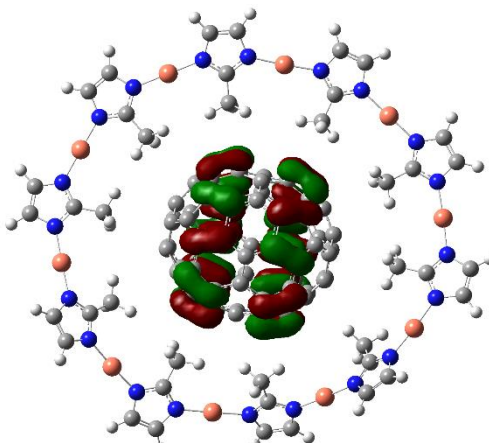
(a) LUMO+5



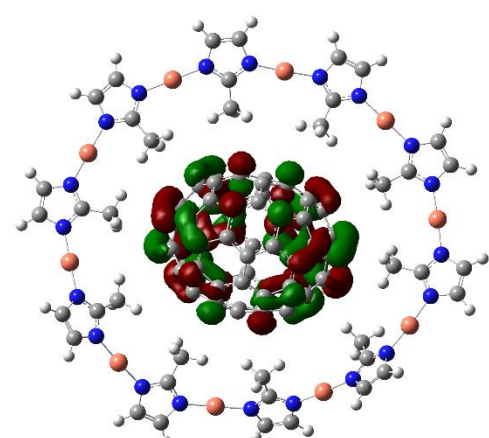
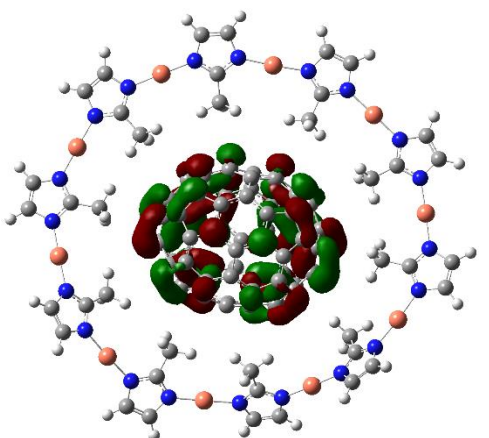
(b) LUMO+4

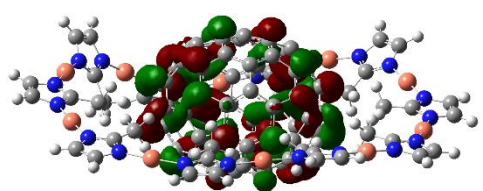


(c) LUMO+3

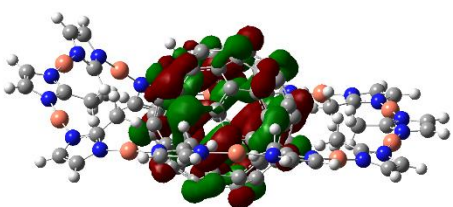


(d) LUMO+2

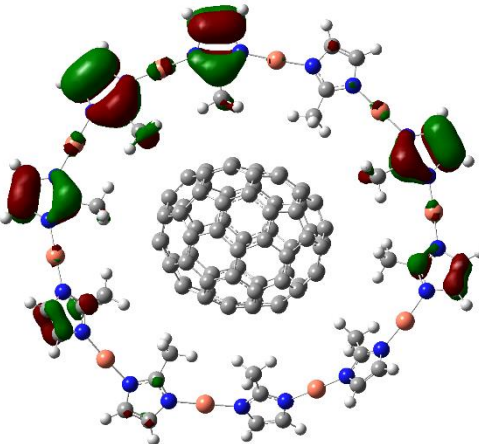
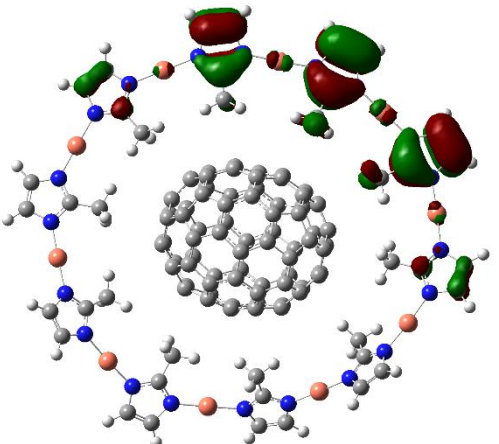




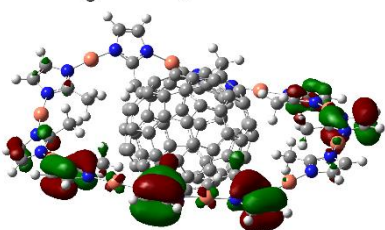
(e) LUMO+1



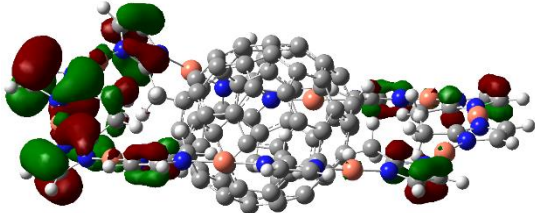
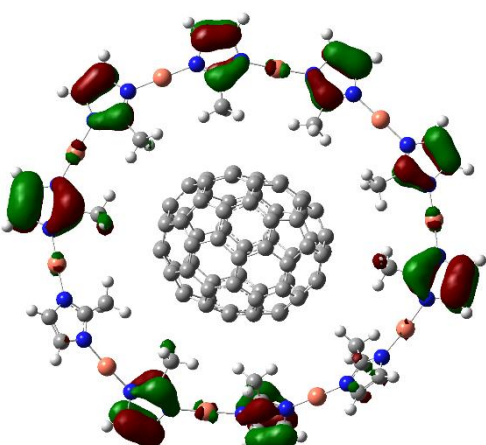
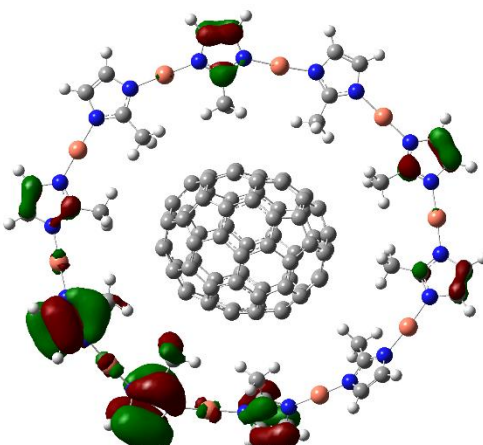
(f) LUMO



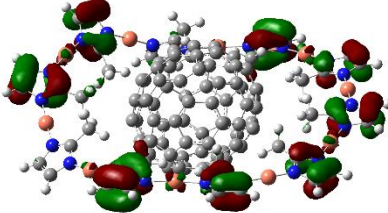
(g) HOMO



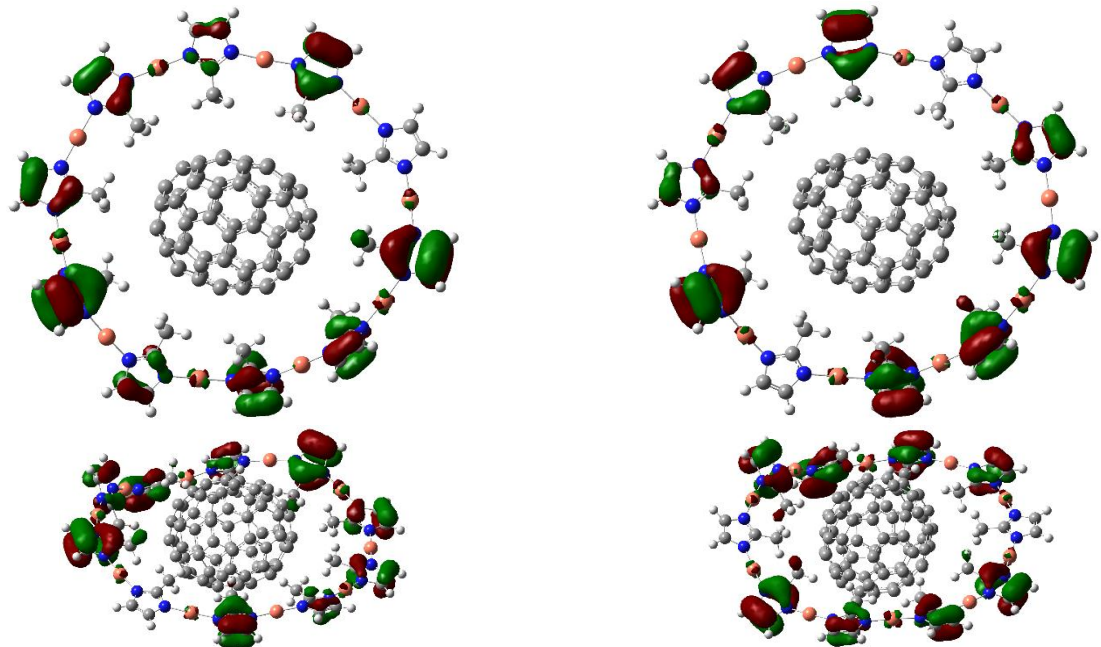
(h) HOMO-1



(i) HOMO-2



(j) HOMO-3



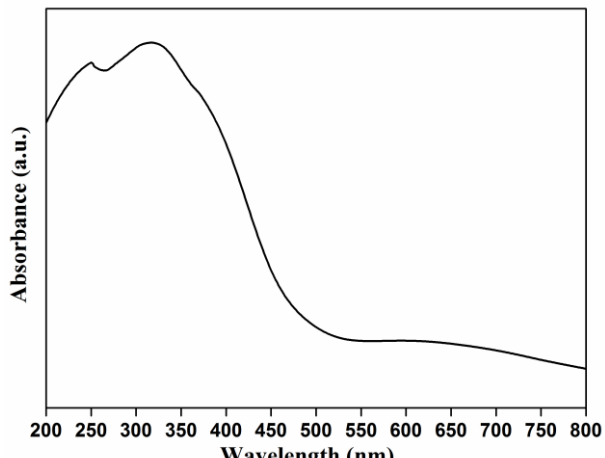
(k) HOMO-4

(l) HOMO-5

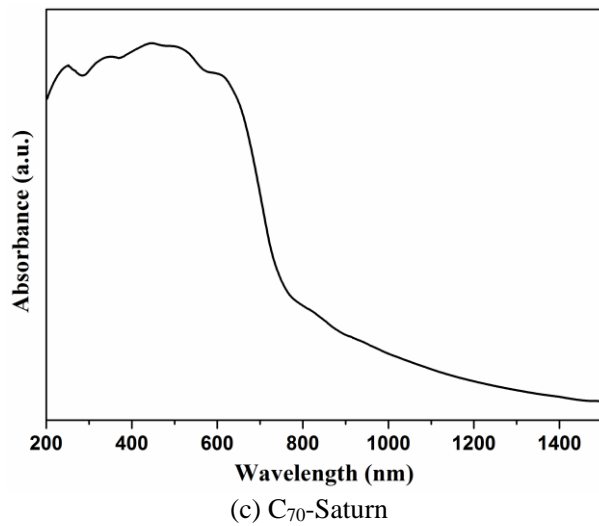
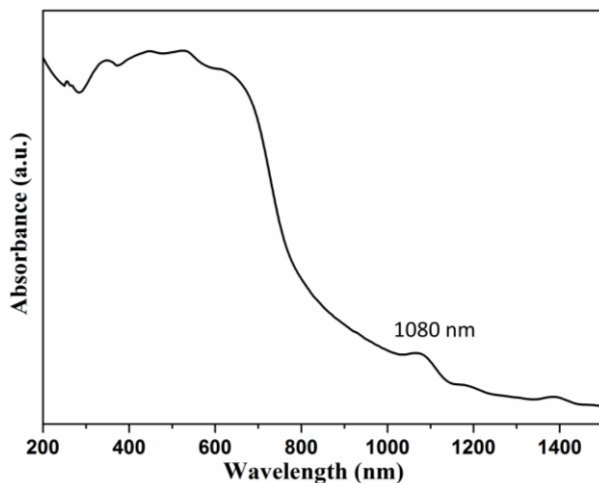
**Fig. S14** Selected molecular orbitals (MOs) at the PBE0 level of theory for the C<sub>70</sub>-Saturn (isovalue = 0.015).

## 4 Femtosecond Transient Absorption (fs-TA)

### 4.1 Reflectance Solid State UV-Vis-NIR Spectra

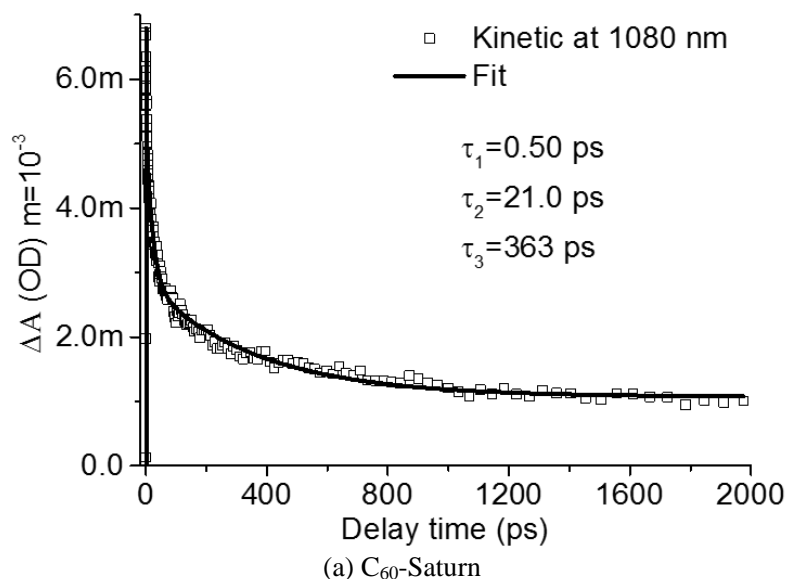


(a) the reported complex [Cu<sub>10</sub>(Mim)<sub>10</sub>]·C<sub>8</sub>H<sub>10</sub>



**Fig. S15** The UV-Vis (a) and UV-Vis-NIR (b, c) diffuse reflectance spectra for the cyclic [Cu<sub>10</sub>(Mim)<sub>10</sub>] $\supset$ C<sub>8</sub>H<sub>10</sub> (a) and the two nano-Saturn complexes (b, c).

#### 4.2 Femtosecond Transient Absorption (fs-TA) Results



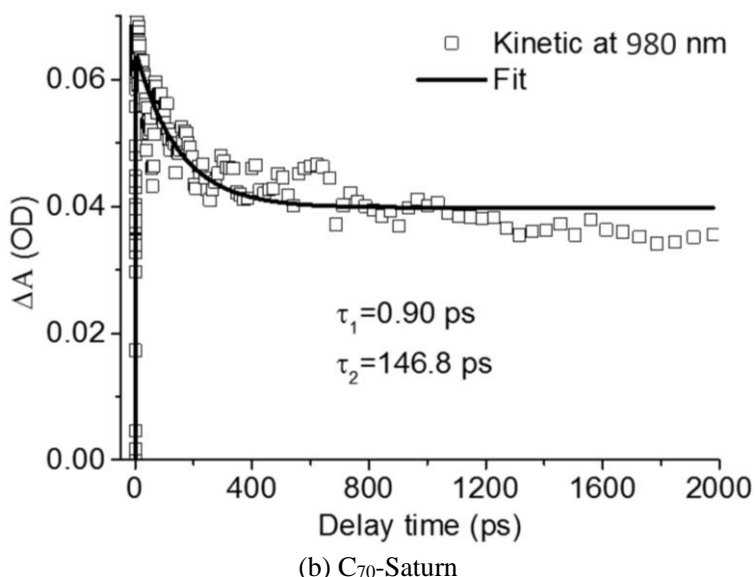


**Fig. S16** Representative decay profiles of the C<sub>60</sub>-Saturn (a) and C<sub>70</sub>-Saturn (b) at probe wavelength  $\lambda = 1080$  nm and 980 nm respectively.

## 5 References

- [1] (a) R. Liang, S.-S. Sun, G. Huang and M.-D. Li, *Chem. Res. Toxicol.*, **2019**, *32*, 613. (b) M. D. Li, N. K. Wong, J. Xiao, R. Zhu, L. Wu, S. Y. Dai, F. Chen, G. Huang, L. Xu, X. Bai, M. R. Geraskina, A. H. Winter, X. Chen, Y. Liu, W. Fang, D. Yang and D. L. Phillips, *J. Am. Chem. Soc.*, **2018**, *140*, 15957.
- [2] G. M. Sheldrick, *Acta Crystallogr., Sect. A: Found. Crystallogr.* **2008**, *64*, 112.
- [3] Y. Yamamoto, E. Tsurumaki, K. Wakamatsu and S. Toyota, *Angew. Chem., Int. Ed.* **2018**, *57*, 8199.
- [4] S. Kigure, H. Omachi, H. Shinohara and S. Okada, *J. Phys. Chem. C* **2015**, *119*, 8931.
- [5] S. Kigure and S. Okada, *Jpn. J. Appl. Phys.* **2015**, *54*, 06FF01.
- [6] H. U. Rehman, N. A. McKee and M. L. McKee, *J. Comput. Chem.* **2016**, *37*, 194.
- [7] H. Shimizu, K. H. Park, H. Otani, S. Aoyagi, T. Nishinaga, Y. Aso, D. Kim and M. Iyoda, *Chem. Eur. J.*, **2018**, *24*, 3793.
- [8] K. Yuan, C.-H. Zhou, Y.-C. Zhu and X. Zhao, *Phys. Chem. Chem. Phys.* **2015**, *17*, 18802.
- [9] I. Gonzalez-Veloso, J. Rodriguez-Otero and E. M. Cabaleiro-Lago, *Phys. Chem. Chem. Phys.* **2018**, *20*, 27791.
- [10] S. Kigure and S. Okada, *J. Phys. Soc. Jpn.* **2013**, *82*, 094717.
- [11] ADF 2016. <http://www.scm.com>.
- [12] G. te Velde and E. J. Baerends, *Phys. Rev. B: Condens. Matter Mater. Phys.*, **1991**, *44*, 7888.
- [13] C. Fonseca Guerra, J. G. Snijders, G. te Velde and E. J. Baerends, *Theor. Chem. Accounts Theor. Comput. Model.*, **1998**, *99*, 391.
- [14] M. J. Frisch, G. W. Trucks, H. B. Schlegel, G. E. Scuseria, M. A. Robb, J. R. Cheeseman, G. Scalmani, V. Barone, B. Mennucci, G. A. Petersson, H. Nakatsuji, M. Caricato, X. Li, H. P. Hratchian, A. F. Izmaylov, J. Bloino, G. Zheng, J. L. Sonnenberg, M. Hada, M. Ehara, K. Toyota, R. Fukuda, J. Hasegawa, M. Ishida, T. Nakajima, Y. Honda, O. Kitao, H. Nakai, T. Vreven, Jr. J.

- A. Montgomery, J. E. Peralta, F. Ogliaro, M. Bearpark, J. J. Heyd, E. Brothers, K. N. Kudin, V. N. Staroverov, R. Kobayashi, J. Normand, K. Raghavachari, A. Rendell, J. C. Burant, S. S. Iyengar, J. Tomasi, M. Cossi, N. Rega, J. M. Millam, M. Klene, J. E. Knox, J.B. Cross, V. Bakken, C. Adamo, J. Jaramillo, R. Gomperts, R. E. Stratmann, O. Yazyev, A. J. Austin, R. Cammi, C. Pomelli, J. Ochterski, R. L. Martin, K. Morokuma, V. G. Zakrzewski, G. A. Voth, P. Salvador, J. J. Dannenberg, S. Dapprich, A. D. Daniels, O. Farkas, J. B. Foresman, J. V. Ortiz, J. Cioslowski and D. J. Fox, GAUSSIAN 09 (Revision A.02), Gaussian, Inc., Wallingford, CT, 2009.
- [15] J. P. Perdew, K. Burke and M. Ernzerhof, Generalized Gradient Approximation Made Simple. *Phys. Rev. Lett.*, **1996**, 77, 3865.
- [16] E. van Lenthe and E. J. Baerends, Optimized Slater-Type Basis Sets for the Elements 1–118. *J. Comput. Chem.*, **2003**, 24, 1142.
- [17] E. van Lenthe, E. J. Baerends and J. G. Snijders, Relativistic Regular Two-Component Hamiltonians. *J. Chem. Phys.*, **1993**, 99, 4597.
- [18] (a) T. Lu and F. W. J. Chen, *Comp. Chem.*, **2012**, 33, 580. (b) Multiwfn manual, version 3.3.8, <http://multiwfn.codeplex.com/>.
- [19] J. P. Perdew, K. Burke and M. Ernzerhof, *Phys. Rev. Lett.*, **1996**, 77, 3865.
- [20] J. P. Perdew, K. Burke and M. Ernzerhof, *Phys. Rev. Lett.*, **1997**, 78, 1396.
- [21] C. Adamo and V. Barone, *Theor. Chem. Acc.*, **2000**, 105(2), 169.
- [22] P. J. Hay and W. R. Wadt, *J. Chem. Phys.*, **1985**, 82, 270.
- [23] J. E. Del Bene, *Chem. Phys. Lett.*, **1983**, 94(2), 213.
- [24] M. von Hopffgarten and G. Frenking, *Wiley Interdiscip. Rev.: Comput. Mol. Sci.*, **2012**, 2, 43.
- [25] K. Morokuma, *J. Chem. Phys.*, **1971**, 55, 1236.
- [26] T. Ziegler and A. Rauk, *Theor. Chim. Acta*, **1977**, 46, 1.
- [27] S. Grimme, *Wiley Interdiscip. Rev.: Comput. Mol. Sci.*, **2011**, 1, 211
- [28] S. Grimme, *J. Comput. Chem.*, **2006**, 27, 1787.
- [29] S. Grimme, *J. Comput. Chem.*, **2004**, 25, 1463.
- [30] S. Grimme, J. Antony, S. Ehrlich and H. Krieg, *J. Chem. Phys.*, **2010**, 132, 154104.
- [31] E. R. Johnson and A. D. Becke, *J. Chem. Phys.*, **2005**, 123, 024101.
- [32] S. Grimme, S. Ehrlich, L. Goerigk, *J. Comput. Chem.*, **2011**, 32, 1456.